

Model-based evaluation of methods to determine C:N and N:P regeneration ratios from dissolved nutrients

Birgit Schneider,¹ Johannes Karstensen, and Andreas Oschlies²

Leibniz-Institut für Meereswissenschaften, Kiel, Germany

Reiner Schlitzer

Alfred Wegener Institut für Polar- und Meeresforschung, Bremerhaven, Germany

Received 12 March 2004; revised 17 January 2005; accepted 16 February 2005; published 15 April 2005.

[1] Four indirect methods to determine carbon and nutrient regeneration ratios in the ocean are applied to results from a physical-biogeochemical model with prescribed element ratios for organic matter (de-)composition. The aim is to test whether these methods are suitable to reproduce $C_{org}:N:P$ element ratios of organic matter remineralization, which in contrast to the real ocean are exactly known in the model framework. The model experiment is carried out using the classical C:N:P Redfield ratio of 106:16:1 for production and decomposition of organic material under preindustrial atmospheric pCO_2 . Two methods rely on predefined end member values, while the others do not. The first method is a simple linear regression of two parameters, neglecting mixing effects, and yields remineralization signals biased by isopycnal tracer gradients induced by contributions of different water masses. The second method is based on multiple linear regression of three parameters, includes mixing of three, but not-prescribed end members. It can, in part, reproduce the prescribed remineralization ratios. However, considerable bias appears as a result of water mass mixing. The third method considers isopycnal mixing of three prescribed end member water masses by using temperature/salinity as conservative tracers on the two density surfaces $\sigma_\theta = 26.8$ and $\sigma_\theta = 27.2$. On the basis of a mixing triangle approach, the method is able to reproduce the regeneration rates best in the low latitudes, where the integrated signal of remineralization is high. The fourth method uses the full set of available parameters to derive mixing fractions and remineralization and is applied to the density range from $\sigma_\theta = 26.8$ to $\sigma_\theta = 27.2$, yielding the best reproduction of prescribed remineralization ratios. As expected, results from the last two methods are sensitive to the choice of end member concentrations. In general, best agreement between modeled and reconstructed ratios is found between $20^\circ N$ and $20^\circ S$ and deviations occur toward the outcrop regions, which we account to the low amount of remineralized material together with uncertainties in prescribed end member values. Our investigation shows how apparent variability of remineralization ratios can be generated through methodological shortcomings only.

Citation: Schneider, B., J. Karstensen, A. Oschlies, and R. Schlitzer (2005), Model-based evaluation of methods to determine C:N and N:P regeneration ratios from dissolved nutrients, *Global Biogeochem. Cycles*, 19, GB2009, doi:10.1029/2004GB002256.

1. Introduction

[2] The carbon, nitrogen, phosphorus (C:N:P) elemental composition of organic matter in the ocean is a key factor for relating carbon and nutrient cycles. Particularly, it is important for calculations of the biotically effected CO_2 uptake by the ocean from nutrient-based biological produc-

tion concepts [Oschlies and Kähler, 2004]. Through the exchange of CO_2 between ocean and atmosphere, the ocean plays a vital role in the global carbon cycle [Siegenthaler and Sarmiento, 1993; Takahashi et al., 1999; Wallace, 2001]. The steady rise of atmospheric CO_2 partial pressure (pCO_2), as a result of changing land use and fossil fuel combustion since the beginning of industrialization, is very likely affecting present and future climate conditions and hence has socio-economic effects and demands political consequences [Intergovernmental Panel on Climate Change (IPCC), 2001].

[3] Intense scientific effort has been undertaken during the last few decades to better understand and quantify the

¹Now at Institut für Geowissenschaften, Kiel, Germany.

²Now at School of Ocean and Earth Science, Southampton Oceanography Centre, Southampton, UK.

underlying fluxes of carbon that partition carbon among atmospheric and oceanic reservoirs. To relate carbon, nitrogen, and phosphorus fluxes by particulate material either direct measurements on particulate material or indirect methods, which reconstruct the particle regeneration signal from changes in dissolved inorganic carbon (DIC) and nutrients, are applied. Long-term direct particle measurements by filter analyzes and sediment trap deployments helped to considerably improve the knowledge of open ocean particle fluxes and their elemental composition. However, there still seem to be conflicting results between direct (particle) measurements and indirect (rem mineralization) estimates, as, for example, $C_{org}:N$ ratios from particulate material are often higher than estimates from regenerated nutrients [Schneider *et al.*, 2003]. One argument favoring the indirect methods, especially in deeper water masses below the permanent thermocline and free from seasonal biases, is the time- and space-integrated view that automatically yields average values. Particle measurements are a more direct estimate of organic material. However, they show large scatter, caused by local, short-term variations associated with single blooms and flux events and may suffer from systematic errors as, for example, dissolved organic matter (DOM) sorption on filters [Moran *et al.*, 1999], or non-ideal trapping efficiency [Buesseler *et al.*, 1994; Scholten *et al.*, 2001], and dissolution of material within the cups of sediment traps [Noji *et al.*, 1999; Kähler and Bauerfeind, 2001].

[4] Most measurement-based estimates of the anthropogenic carbon content in the ocean rely on a rather simple concept subtracting the effect of organic matter remineralization from in situ dissolved inorganic carbon (DIC) and nutrient concentrations. However, this also requires knowledge about carbon and nutrient remineralization rates. An often used strategy to relate carbon and nutrient element ratios is the implementation of the Redfield ratio (RR) [Redfield *et al.*, 1963], which assumes a constant molar ratio for $C_{org}:N:P:-O_2$ of 106:16:1:-138 for both particle formation and regeneration. However, more recent indirect methods have repeatedly been used to challenge the RR concept for export and remineralization of organic matter [e.g., Takahashi *et al.*, 1985; Minster and Boulaïdid, 1987; Anderson and Sarmiento, 1994; Shaffer *et al.*, 1999; Hupe and Karstensen, 2000; Li and Peng, 2002]. As different authors tend to find different and sometimes contradictory remineralization ratios, concerning, for example, basin-wide and vertical patterns, it is not entirely clear to what extent the results are affected by methodological artifacts. The indirect methods are applied to hydrographic data sets of DIC, nutrient (NO_3 , PO_4), and oxygen (O_2) distributions to identify remineralization-induced changes in nutrient concentrations in carefully selected water masses. Conceptual difficulties are assumptions about water mass transport, which is supposed to occur mainly along isopycnals/neutral density surfaces, and often neglect diapycnal/dianeutral mixing. The mixing of different water masses is often resolved for two or three end member values only. One study explicitly considered various vertical transport processes [Shaffer *et al.*, 1999] and found a pronounced vertical fractionation of the elements.

[5] A further pitfall for studies on isopycnals/neutral density surfaces could be the incorrect linear interpolation of the observational data onto the “spreading surfaces,” the importance of which will be demonstrated later in our study. Furthermore, a potential source of error is the definition of end member characteristics [e.g., Takahashi *et al.*, 1985; Minster and Boulaïdid, 1987; Hupe and Karstensen, 2000]. End members have to be defined in the particular formation region of a water mass; otherwise the data may already be composed by mixing of a number of end members. It is, however, difficult to identify formation regions, and furthermore, these regions may not always be included in the particular data set. Those studies, that tried to overcome explicit end member definition, had at least to limit the number of potential end members (i.e., to not more than three) [e.g., Anderson and Sarmiento, 1994; Shaffer *et al.*, 1999; Li and Peng, 2002]. Finally, further complications occur from contamination with anthropogenic CO_2 , which leads to a reduction of apparent carbon to nutrient remineralization ratios [Gruber, 1998; Körtzinger *et al.*, 2001].

[6] In this study we test four different indirect methods for the determination of remineralization ratios for dissolved inorganic carbon (DIC) and the nutrients nitrate (NO_3) and phosphate (PO_4) in the framework of a coupled biogeochemical circulation model that is tuned to closely reproduce global DIC and nutrient measurements. Even though models have to simplify processes in certain ways, they are internally consistent in their assumptions and, in this respect, represent an ideal data set. The model used in this study provides long-term averages of T, S, DIC, and nutrient distributions and does not resolve seasonal or interannual variability. Furthermore, nitrogen fixation and denitrification do not exist in the model. The experiments are run into steady state under preindustrial conditions, thus avoiding any anthropogenic perturbation of the simulated DIC field. Production and remineralization of organic matter are forced to exactly reproduce the classical RR of $C_{org}:N:P$ (106:16:1). Within this model framework we want to (1) find out whether indirect methods of nutrient analyzes can identify the correct remineralization ratio (here the classical RR) and (2) identify the critical aspects of the different indirect methods and the optimal conditions/regions for the application of the different methods.

2. Model Data

[7] The various methods used to derive remineralization ratios are applied to the model output of the AWI Adjoint Model for Oceanic Carbon Cycling (AAMOC) [Schlitzer, 2000, 2002]. It is a 3-D ocean circulation model simulating global distributions of dissolved inorganic carbon (DIC), nitrate (NO_3), phosphate (PO_4), oxygen (O_2), total alkalinity (TALK), and dissolved organic matter (DOM) in addition to the hydrographic parameters temperature (T) and salinity (S). For our study we used the output from an AAMOC model run with constant flow field, taken from a previous optimization experiment, where water mass transports and tracer distributions (T, S, DIC, NO_3 , PO_4 , O_2 , and TALK) are close to observations. Particle production and remineralization are not simulated explicitly, but occur as sinks and

sources of DIC and nutrients using Suess/Martin-type equations [Suess, 1980; Martin *et al.*, 1987]. There is gas exchange at the sea surface for CO₂ and O₂. DOM production equals POM production in both amount and elemental composition. Formation and dissolution of calcium carbonate (CaCO₃) affect the concentration of dissolved inorganic carbon ($\Delta\text{DIC}_{\text{CaCO}_3}$), which are considered by changes in alkalinity (ΔTALK) and corrected for effects by nitrate (ΔNO_3):

$$\Delta\text{DIC}_{\text{CaCO}_3}[\text{mol}] = (\Delta\text{TALK} + \Delta\text{NO}_3) : 2[\text{mol}]. \quad (1)$$

[8] In the current study, the model experiment represents preindustrial steady state with an atmospheric pCO₂ of 278 ppm. To reach equilibrium, the model is integrated for 5000 years, until there is no net gas exchange of CO₂ between ocean and atmosphere. Particle fluxes as well as production and decay of DOM are implemented following the classical RR for C_{org}:N:P of 106:16:1, achieving a global carbon export production of 10 Gt C [Schlitzer, 2002]. Only for the O₂:P ratio a nonclassical Redfield value of -175 [Takahashi *et al.*, 1985] is applied. Note that because of the model's neglect of any non-Redfield processes like denitrification or N₂ fixation, the optimization routine may make up for this neglect of biological processes by unrealistic adjustments to the circulation field. We investigate AAMOCC model results from the Atlantic Ocean for the depth interval between $\sigma_\theta = 26.8 \text{ kg m}^{-3}$ and 27.2 kg m^{-3} , representing the lower thermocline.

3. Methods

3.1. Linear Regression Methods Without Predefined End Member Characteristics

3.1.1. Two Parameter Linear Regression

[9] The first method (M1a) infers ratios of carbon and nutrient remineralization for two isopycnal surfaces by regressing the total concentrations of DIC against NO₃ and PO₄ along an isopycnal surface. The interpolation to the two target isopycnals 26.8 kg m^{-3} and 27.2 kg m^{-3} is done by constructing at each grid point high vertical resolution ($\Delta z = 1 \text{ m}$) profiles of all tracers using an Akima spline [Akima, 1970] and subsequently interpolating to density. This procedure minimizes interpolation errors that occur as a result of the nonlinearity of the equation of state. Such an error can be a serious problem when using data with a coarse vertical resolution in comparison to the vertical gradients of a parameter. The regression uses the reduced major axis approach [Pearson, 1901], which takes into account variability of both variables simultaneously. We refer to the method as the regression method (M1a). Although it has been shown that this method suffers from the neglect of mixing effects [e.g., Takahashi *et al.*, 1985], we include it in our study to demonstrate the sensitivity of so derived ratios through mixing effects. It assumes that all variability in inorganic tracer concentrations on a given isopycnal arises exclusively from biological processes,

$$(C_i : N)_r^{M1a} = (\text{DIC} - \text{DIC}_0) : \Delta\text{NO}_3, \quad (2)$$

where $(C_i : N)_r$ is the estimated remineralization ratio of total carbon versus nitrogen and DIC and NO₃ are the absolute concentrations of dissolved inorganic carbon and nitrate. This method assumes a single DIC₀ value for NO₃ = 0 (or any other NO₃ value), which implies that differences in DIC and nutrient end member concentrations in the outcrop regions and subsequent mixing of different end members along isopycnals are not considered.

[10] The reduced major axis fit regressions of DIC versus NO₃ and of NO₃ versus PO₄ are carried out on each isopycnal separately for each of the North and South Atlantic basins. To correct changes in the DIC concentrations owing to CaCO₃ dissolution ($\Delta\text{DIC}_{\text{CaCO}_3}$) we utilize the results from Chung *et al.* [2003] (see equations (6) and (7) below). In brief, Chung *et al.* [2003] calculated a preformed alkalinity based on a multiple regression analysis considering salinity and nitrate data. The preformed alkalinity is utilized to derive a $\Delta\text{DIC}_{\text{CaCO}_3}$ considering apparent oxygen utilization, alkalinity, and remineralization ratios. For our application the AAMOCC model prescribed RR are used.

3.1.2. Multiple Linear Regression

[11] The second method (M1b) is based on a multiple linear regression [Li and Peng, 2002]. Basically, it is a reformulation of the concept of a quasi-conservative tracer [Broecker, 1974], composed from oxygen and a nutrient. For nitrate and oxygen the quasi-conservative tracer, often called "NO," is

$$'NO' = \text{O}_2 + r_n \cdot \text{NO}_3. \quad (3)$$

[12] A basic assumption is that the remineralization ratio r_n is constant within the region of investigation, so that NO should behave like other conservative tracers as temperature and salinity. Li and Peng [2002] accordingly reformulated NO as

$$\text{NO} = \alpha_0 + \alpha_1 \cdot T + \alpha_2 \cdot S = \text{O}_2 + r_n \cdot \text{NO}_3. \quad (4)$$

[13] Here, factors ($\alpha_1, \alpha_2, \alpha_3$) carry the linear mixing of three end member characteristics in temperature, salinity, and nitrate under the assumption of mass conservation. Similar equations can be written for phosphate and carbon (see work of Li and Peng [2002] for further details). To derive the remineralization ratios (r_n) a multiple linear regression is performed. Although a prerequisite for the analysis is that the data to be analyzed are composed of a maximum of three end members, no specific end member characteristics have to be defined. Li and Peng [2002] utilized temperature and salinity data to identify regions composed of a maximum of three end members.

[14] We will apply this method in two ways. First we use the AAMOCC model output interpolated to the isopycnals 26.8 kg m^{-3} and 27.2 kg m^{-3} as explained above. Second, all model data for the Atlantic Ocean between 40°N and 40°S, but in the regional and temperature/salinity boundaries given by Li and Peng [2002] is analyzed.

3.2. Mixing Methods With Predefined End Member Characteristics

[15] In contrast to the two regression methods above, two methods that explicitly account for the effects of mixing of

water masses with predefined end member characteristics in DIC, nutrients, and temperature and salinity are applied to the model data. In principle, it is assumed that any value of a conservative parameter (as potential temperature and salinity) at a given location results only from mixing of waters represented through end member characteristics, while nonconservative parameters, such as nutrients and carbon, are affected by the same mixing, but in addition carry a change through biogeochemical processes [Karstensen and Tomczak, 1998]. Because production of organic matter requires light as energy source, beneath the euphotic zone only remineralization of organic matter has to be taken into account.

[16] In our study we use two different ways to isolate the mixing from the remineralization signal. Both approaches are based on an extension of the optimum multiparameter (OMP) analysis [Karstensen and Tomczak, 1998], but use it with different degrees of complexity. The first one (M2a) derives the mixing ratios only from conservation of T and S. This method is closely related to the nutrient data analysis of Takahashi *et al.* [1985]. In contrast to the classical mixing triangle [Helland-Hansen, 1918], however, the water mass fractions are constrained to be positive or zero only. This is realized through a non-negative least square fit [Lawson and Hanson, 1974]. Briefly, M2a assumes quasi-isopycnal mixing of two end members of northern and southern origin, permitting diapycnal injection of water from the Mediterranean. As only three end members are used, the application is restricted to isopycnal surfaces rather than being applicable to a 3-D volume. For the analysis, we use the AAMOC model output interpolated to the isopycnals 26.8 kg m^{-3} and 27.2 kg m^{-3} as explained above.

[17] The second approach (M2b) applies the OMP analysis using all tracers in one set of equations of the following form [Hupe and Karstensen, 2000]:

$$\begin{aligned}
 f_1 T_1 + \dots + f_n T_n + 0 + 0 &= T_{\text{obs}} + R_T, \\
 f_1 S_1 + \dots + f_n S_n + 0 + 0 &= S_{\text{obs}} + R_S, \\
 f_1 O_{2,1} + \dots + f_n O_{2,n} - r_{O/P} \Delta P + 0 &= O_{2,\text{obs}} + R_{O_2}, \\
 f_1 PO_{4,1} + \dots + f_n PO_{4,n} + r_{P/P} \Delta P + 0 &= PO_{4,\text{obs}} + R_{PO_4}, \\
 f_1 NO_{3,1} + \dots + f_n NO_{3,n} + r_{N/P} \Delta P + 0 &= NO_{3,\text{obs}} + R_{NO_3}, \\
 f_1 DIC_1 + \dots + f_n DIC_n + r_{C_{\text{org}}/P} \Delta P + \Delta C_{CaCO_3} &= DIC_{\text{obs}} + R_{DIC}, \\
 f_1 TALK_1 + \dots + f_n TALK_n - r_{N/P} \Delta P + 2\Delta C_{CaCO_3} &= TALK_{\text{obs}} + R_{TALK}, \\
 f_1 + \dots + f_n + 0 + 0 &= 1 + R_{\Sigma}.
 \end{aligned} \tag{5}$$

[18] This set of equations contains: the effect of mixing, expressed in terms of mixing fractions (f) of n different end member characteristics. The same fractions appear for each tracer. Next, there are the joint changes in nutrients, DIC, and oxygen due to remineralization/respiration, referenced by the appropriate (a priori unknown) element ratio to the amount of remineralized phosphate (ΔP). The link between the different tracers is based on a set of first guess remineralization ratios ($r_{N/P}$, etc.), which are not part of the solution. Incorporating those first-guess remineralization

ratios into the solution would turn the system into a nonlinear one as in the work of Anderson and Sarmiento [1994]. Finally, the contribution which stems from the calcium carbonate dissolution (ΔC_{CaCO_3}) is considered for DIC and alkalinity only.

3.2.1. Defining End Member Characteristics

[19] For the mixing methods (M2a and M2b), end member values or source water types (SWT) of conservative and nonconservative variables have to be defined first. Choosing SWT values is always a delicate task as the results may be sensitive to their choice. For biogeochemical studies it is advantageous that the SWT are defined either in the outcrop regions or where the respective water mass enters an ocean basin. Utilizing interior points as basis of definition, SWTs are likely already a mixing product of other SWTs from other regions or different stages of biogeochemical cycling. We will return to this point when discussing the results from the Li and Peng [2002] multiple regression method (M1b).

[20] Different approaches have been used in the past to define SWTs. One possibility is to use existent water mass definitions [e.g., Emery and Meincke, 1986]. As the historical definitions are often based on temperature and salinity values only, additional parameters, as, for example, nutrients and DIC, associated with these water masses, have to be determined. In general, the historical definitions do not always use data from water mass formation areas.

[21] Another approach uses statistical methods, like cluster analysis [e.g., You and Tomczak, 1993] to identify water masses by assuming that the unmixed water appears as a cluster of points in different parameter spaces simultaneously. As with the historical definitions, one disadvantage of this approach is that the observational data may not have been collected in the water mass formation areas.

[22] Our SWT definition is done in two stages. The first stage is to identify the formation areas and the second is to pick out the SWT data in the formation regions. Locating the formation areas of the water masses is done by utilizing the apparent oxygen utilization (AOU), the difference between observed oxygen and the saturation value [Weiss, 1970]. The most recently ventilated water is more saturated in oxygen, hence it has a lower AOU than “older” waters. As we use the AAMOC model data, a further constraint is that only data below the second vertical grid cell (below 133 m depth) are used, as the AAMOC model prescribes remineralization to start here.

[23] The spatial distribution of the source water formation regions agrees with current thinking on the thermocline ventilation of the North and South Atlantic Ocean [Marshall *et al.*, 1993; Karstensen and Quadfasel, 2002]. Ventilation sites are at the poleward side of the subtropical gyres and in the western boundary current regions (Figure 1). The T/S pairs associated with low AOU values (below $40 \mu\text{mol kg}^{-1}$) (Figure 2) show that the Atlantic main thermocline is ventilated by at least two different Central Water masses [Sverdrup *et al.*, 1942]: North Atlantic Central Water (NACW) and South Atlantic Central Water (SACW). The SACW is, on isopycnals, about 1.2 psu less saline and about 5°C colder than the NACW. Both merge at temperatures less than 4°C covering a wide range of salinities (and densities). In the North Atlantic an additional type of water modifies the

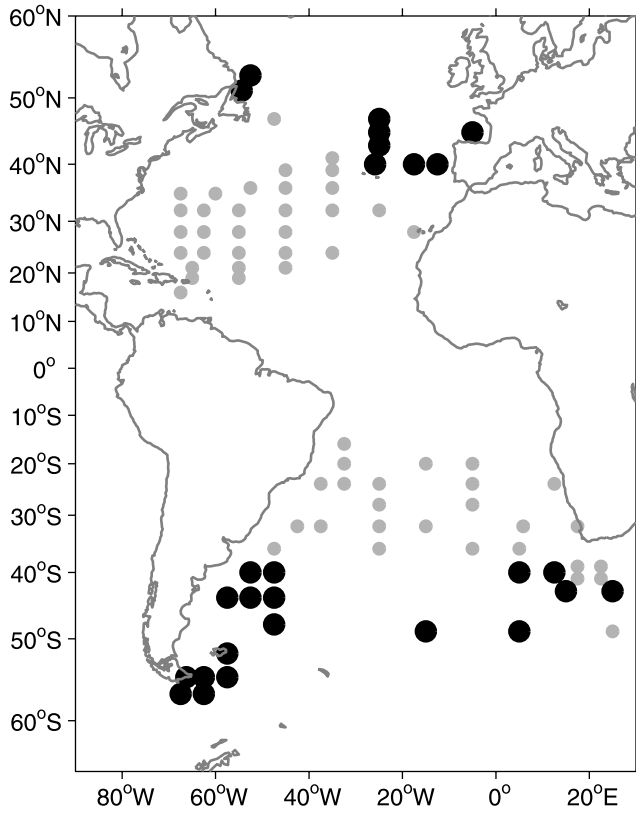


Figure 1. Map of the AOU (apparent oxygen utilization) derived ventilation regions in the AAMOCC model Atlantic Ocean. Only data in the depth range where remineralization is active (>133 m) with AOU values lower than $40 \mu\text{mol kg}^{-1}$ are considered. The black symbols denote ventilation areas in the density range from $\sigma_{\Theta} = 26.8 \text{ kg m}^{-3}$ to $\sigma_{\Theta} = 27.2 \text{ kg m}^{-3}$, which this study refers to; shaded symbols show all other ventilation areas.

thermocline waters through mixing, the high-salinity water from the Mediterranean Sea (MW) with a core density of about 27.6 kg m^{-3} . The MW mixes diapycnally into the ambient water masses, as can be identified through the triangle shape of T/S pairs from its vertex at about $10.51^{\circ}\text{C}/36.08 \text{ psu}$.

[24] The next stage is to define the SWT characteristics. We pick out an upper and lower temperature and salinity SWT for each Central Water plus one for the MW guided by temperature and salinity with lowest AOU values. Then corresponding oxygen, nutrient, carbon, and alkalinity values are picked out from the AAMOCC model data (Figure 2).

[25] The full set of five SWT values (Table 1) is used for the OMP analysis (M2b). For the mixing triangle approach (M2a) the SWT values of the Central Waters (NACW and SACW) are interpolated to the respective isopycnals 26.8 kg m^{-3} and 27.2 kg m^{-3} , as it was explained for M1a. Considering the single SWT of the MW, this resulted in three end members for each “isopycnal” (see Table 2). One may emphasize that the M2a approach is not a strict isopycnal mixing approach as the MW has its SWT in denser water than the two isopycnals analyzed with M2a. However, it is not

possible to unambiguously define a single MW SWT for the 26.8 kg m^{-3} or 27.2 kg m^{-3} isopycnal.

[26] M2a assumes linear mixing, while the isopycnals are nonlinear (see Figure 2). In the worst case (on the isopycnal 27.2 kg m^{-3}) the isopycnal is 0.3°C warmer and 0.03 psu fresher compared to the linear mixing line between NACW and SACW. A “classical” mixing triangle approach [Helland-Hansen, 1918] without a non-negative least square fit would result in 53% SACW, 60% NACW, and a physically meaningless negative contribution of MW of -10% . Mathematically, a negative contribution of cold and saline MW allows for the apparent freshening and warming through the linear mixing approach. However, using the non-negative least square fit, as is done in our analysis, MW contributes 0% and SACW and NACW contribute 53% and 46%, respectively. These “linearized” fractions are similar (within 1%) to what one would obtain calculating fractions along a density line. Note that if the MW was a warm and saline water mass, it might fully compensate for the apparent warming and freshening as a result of the linear approach.

3.2.2. Determination of Mixing Fractions and Regeneration Rates From AAMOCC Model Data

[27] The M2a approach is applied to AAMOCC model data interpolated to the two target isopycnals, 26.8 and 27.2 kg m^{-3} . All T and S data points on the respective isopycnals are analyzed for the mixing fractions (f) of NACW, SACW, and MW. These mixing fractions are then combined with the SWT of DIC and nutrients on the target isopycnal (Table 1) to compose “mixing-only” preformed values of DIC (DIC_p) and nutrients ($\text{NO}_{3,p}$, $\text{PO}_{4,p}$) for each data point. Subtracting these mixing-only preformed values from the actual model data ($\text{DIC}_{\text{model}}$, $\text{NO}_{3,\text{model}}$, $\text{PO}_{4,\text{model}}$) gives the changes in each tracer through remineralization.

[28] To achieve the organic carbon remineralization (ΔC_{org}), one has to correct the total carbon remineralization (ΔDIC) for CaCO_3 dissolution. This is done using the TALK and NO_3 changes during remineralization,

$$\Delta C_{\text{org}} = \Delta \text{DIC} - (\Delta \text{TALK} + \Delta \text{NO}_3) : 2, \quad (6)$$

where

- ΔC_{org} organic carbon remineralization;
- ΔDIC total remineralized carbon ($\Delta \text{DIC} = \text{DIC}_{\text{model}} - \text{DIC}_p$);
- ΔTALK remineralized alkalinity ($\Delta \text{TALK} = \text{TALK}_{\text{model}} - \text{TALK}_p$);
- ΔNO_3 remineralized nitrate ($\Delta \text{NO}_3 = \text{NO}_{3,\text{model}} - \text{NO}_{3,p}$).

[29] The $C_{\text{org}}:\text{N}$ and $\text{N}:\text{P}$ remineralization ratios are then calculated as follows:

$$(C_{\text{org}} : \text{N})_r^{M2a} = \Delta C_{\text{org}} : \Delta \text{NO}_3 \quad (7)$$

$$(N : \text{P})_r^{M2a} = \Delta \text{NO}_3 : \Delta \text{PO}_4, \quad (8)$$

where ΔPO_4 is remineralized phosphate ($\Delta \text{PO}_4 = \text{PO}_{4,\text{model}} - \text{PO}_{4,p}$). The M2b method is applied to the interpolated data on

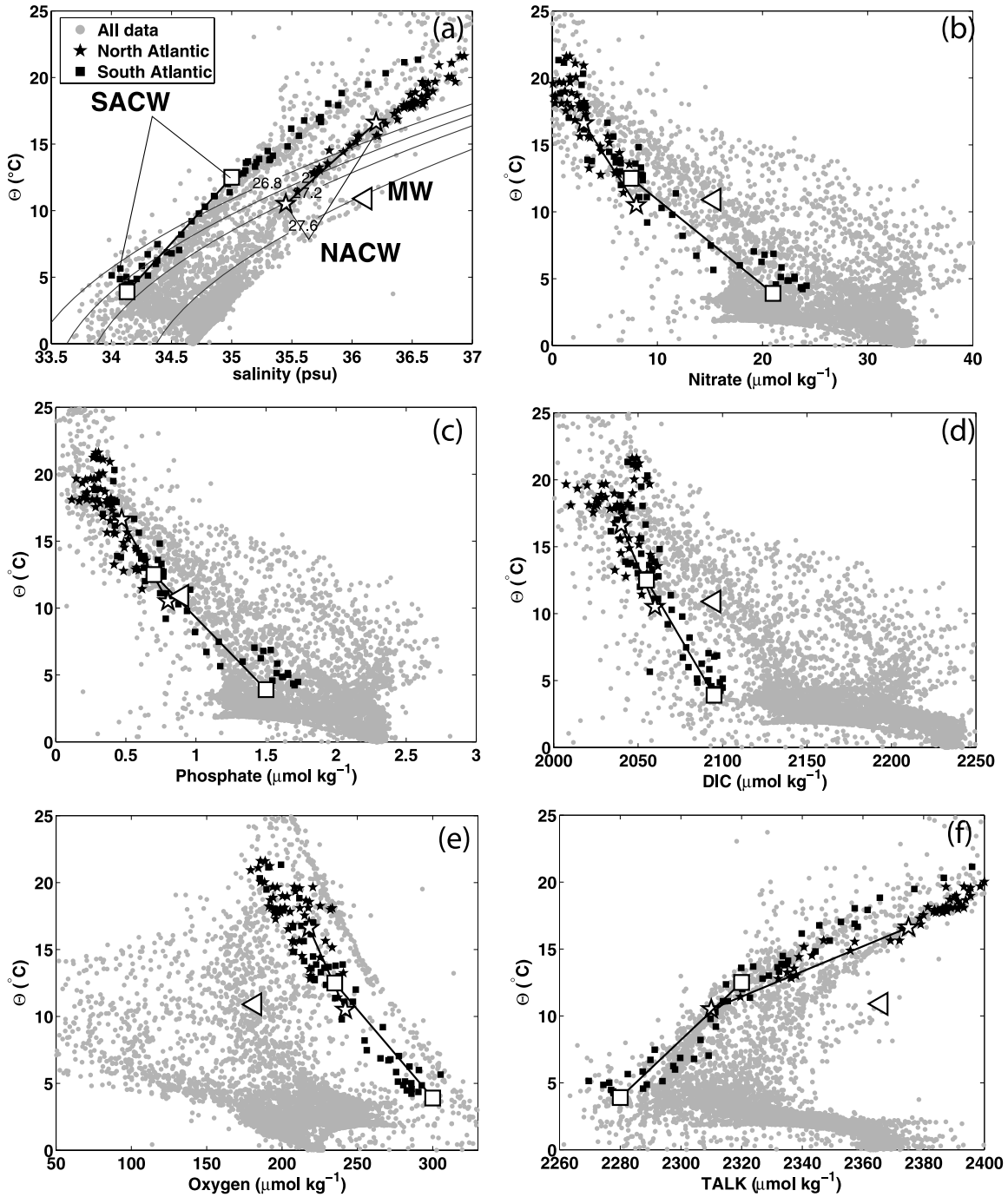


Figure 2. Source waters as determined for the M2b method, for (a) T and S, (b) nitrate, (c) phosphate, (d) DIC, (e) oxygen, and (f) total alkalinity. The shaded dots show all data for the AAMOC Atlantic model output; black symbols show values with AOU below $40 \mu\text{mol kg}^{-1}$. Symbols represent the determined SWT characteristics. NACW, North Atlantic Central Water; SACW, South Atlantic Central Water; MW, Mediterranean Water.

the two isopycnals and in addition to all data in the density range 26.8 to 27.2 kg m^{-3} without further interpolation. M2b determines for each data point in a single step the mixing fractions (f), the amount of remineralized phosphate (ΔP), and the calcium carbonate dissolution (ΔC_{CaCO_3}). Note that the first guess remineralization ratios ($r_{\text{parameter}/P}$) are constant

during the analysis run. To determine a set of “new” regeneration ratios from the solution of the system of equations (5), we proceed as follows: A mixing-only preformed value is calculated from the SWT values and the mixing fractions. Adding the ΔC_{CaCO_3} loss and subtracting the result from the in situ model data gives the amount of

Table 1. Source Waters for Method M2b (Full OMP Analysis)^a

	T, °C	S	DIC, $\mu\text{mol kg}^{-1}$	NO_3 , $\mu\text{mol kg}^{-1}$	PO_4 , $\mu\text{mol kg}^{-1}$	O_2 , $\mu\text{mol kg}^{-1}$	TALK, $\mu\text{mol kg}^{-1}$
NACW							
Upper	16.61	36.20	2040	3.0	0.47	218	2375
Lower	10.50	35.45	2060	8.0	0.80	242	2310
SACW							
Upper	12.50	35.00	2055	7.5	0.70	235	2320
Lower	3.90	34.13	2101	21.0	1.51	300	2290
MW	10.51	36.08	2098	16.0	0.85	179	2366
Noise	0.01	0.05	1	0.1	0.01	1	1

^aThe Mediterranean water mass characteristic is optimized via random noise experiments (see text for further details).

remineralized material for each tracer including the residuals of the individual tracer (R_x). A remineralization ratio for each (model) observation is finally derived by relating the thus calculated remineralized material of the tracers accordingly.

4. Results

[30] As the aim of the current study is to test different methods in their ability to reconstruct the known ratio of remineralization products used in the AAMOCC model, the applied methods can be compared in their results concerning (1) the reconstruction of the AAMOCC underlying remineralization ratios (106:16:1:–175 for C_{org} :N:P:O₂), (2) the amount of dissolved CaCO₃, (3) the water mass fractions of NACW, SACW, and MW (M2a and M2b only), and (4) the amount of remineralized material (ΔPO_4 , ΔC_{org}) (M2a and M2b only).

4.1. Linear Regression Method (M1a)

[31] As there is a distinct influence of southern water masses across the equator until 15°N, which will also be confirmed later by the mixing methods, we separate the North and South Atlantic regimes at 15°N. In the North Atlantic the $(C_i:N)_r$ along both isopycnals gives values of 5.6 (26.8 kg m⁻³; $r = 0.984$; 27.2 kg m⁻³; $r = 0.987$) which is distinctly lower than the C_{org} :N regeneration ratio of 6.6 used in the AAMOCC model (Figure 3, Table 3). For the South Atlantic we obtain higher $(C_i:N)_r$ regressions of 7.1 ($r = 0.969$) on 26.8 kg m⁻³ and of 9.0 ($r = 0.957$) on 27.2 kg m⁻³. Displaying the regression slopes versus latitude confirms the picture of lower $(C_i:N)_r$ in the North and higher ratios in the South Atlantic with significantly larger deviations on the deeper isopycnal (Figure 3). However, in the model as well

as in the real ocean changes in the DIC, concentrations will also be caused by CaCO₃ dissolution. Therefore the regenerated DIC has to be corrected by the effect of CaCO₃-dissolution, using changes in alkalinity and nitrate (equation (1)). By using linear regression slopes as in M1a, this leads to even higher organic carbon regeneration rates than total carbon remineralization rates, caused by inappropriate mixing assumptions of this method. Thus, for a better correction, we apply the local CaCO₃-correction as determined by *Chung et al.* [2003]. This, however, yields only slightly improved results for C_{org} :N regeneration ratios (Figure 3). Merely the C_{org} :N regeneration ratios for the South Atlantic on the 26.8 kg m⁻³ isopycnal match the modeled C:N regeneration ratios after correction.

[32] The slope of the NO_3 : PO_4 on the 26.8 kg m⁻³ isopycnal perfectly matches the prescribed N:P ratio of 16 in both Atlantic basins (North, $r = 0.999$; South, $r = 1$), and even the y-intercepts are only slightly different (Table 3). On the 27.2 isopycnal there are slight deviations with a slope of 15.8 in the North Atlantic ($r = 0.999$) and 16.1 in the South Atlantic ($r = 1$). Plotting the NO_3 : PO_4 regression slopes versus latitude reveals some deviations in the North Atlantic, but a perfect match in the South Atlantic for both isopycnal (Figure 4). This indicates that the NO_3 : PO_4 ratio seems to be a rather robust feature for the AAMOCC Atlantic Ocean, at least on the two isopycnals considered. Note, however, that the AAMOCC model does not allow for nitrogen fixation or denitrification which, in reality, affect the NO_3 : PO_4 ratio and therefore would be difficult to distinguish from non-Redfield remineralization ratios [*Gruber and Sarmiento*, 1997].

[33] In summary, strictly using the regression method M1a, we are not able to reconstruct the AAMOCC prescribed C_{org} :N remineralization ratio satisfactorily. This

Table 2. Source Water Mass Characteristics for Method M2a^a

	T, °C	S	DIC, $\mu\text{mol kg}^{-1}$	NO_3 , $\mu\text{mol kg}^{-1}$	PO_4 , $\mu\text{mol kg}^{-1}$	O_2 , $\mu\text{mol kg}^{-1}$	TALK, $\mu\text{mol kg}^{-1}$
$\sigma_\theta = 26.8 \text{ kg m}^{-3}$							
NACW	14.40	35.93	2045	6.5	0.59	222	2341
SACW	9.20	34.67	2082	13.2	1.05	233	2312
$\sigma_\theta = 27.2 \text{ kg m}^{-3}$							
NACW	10.50	35.43	2050	6.5	0.60	240	2335
SACW	3.50	34.20	2090	20.5	1.50	311	2292
$\sigma_\theta = 27.6 \text{ kg m}^{-3}$							
MW	10.51	36.08	2098	16.0	0.85	179	2366

^aEssentially, the source waters from Table 1 are interpolated to the isopycnals 26.8 kg m⁻³ and 27.2 kg m⁻³.

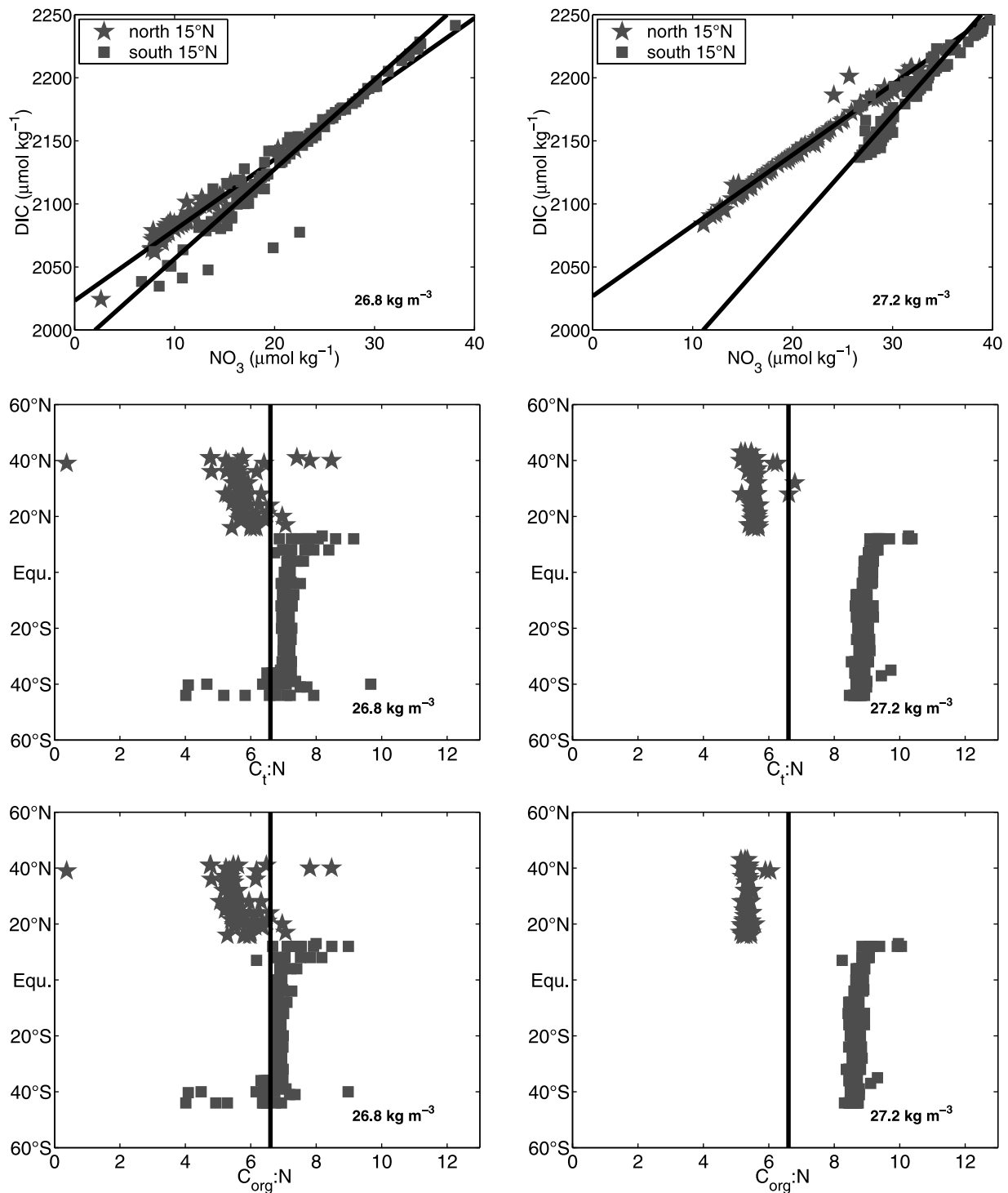


Figure 3. (top) Regression lines (M1a) of modeled total inorganic carbon (DIC) versus NO_3 concentrations from the (left) $\sigma_\theta = 26.8 \text{ kg m}^{-3}$ and (right) $\sigma_\theta = 27.2 \text{ kg m}^{-3}$ isopycnals. The black lines show the slopes of the regression lines (reduced major axis) for data from the North Atlantic (stars) and South Atlantic (squares), respectively. (middle) $C_t:N$ plotted versus latitude; note different scaling than the N:P ratios and other C:N ratios in following plots. (bottom) $C_{org}:N$ obtained after correcting $C_t:N$ for the effect of CaCO_3 dissolution using the method of Chung *et al.* [2003].

Table 3. Regressions (Reduced Major Axis) of Total Inorganic Carbon (DIC) Versus Nitrogen (NO_3) and Nitrogen Versus Phosphorus (PO_4) in the North (North of 15°N) and South (South of 15°N) Atlantic on the Two Isopycnals $\sigma_\theta = 26.8 \text{ kg m}^{-3}$ and $\sigma_\theta = 27.2 \text{ kg m}^{-3}$, Number of Samples (n), and Correlation Coefficient (r)

	Regression Equation	n	r
<i>DIC Versus Nitrogen</i>			
$\sigma_\theta = 26.8 \text{ kg m}^{-3}$			
North Atlantic	$(\text{C}_t:\text{N})_r = 5.6 \cdot \text{NO}_3 + 2023$	74	0.984
South Atlantic	$(\text{C}_t:\text{N})_r = 7.1 \cdot \text{NO}_3 + 1986$	129	0.969
$\sigma_\theta = 27.2 \text{ kg m}^{-3}$			
North Atlantic	$(\text{C}_t:\text{N})_r = 5.6 \cdot \text{NO}_3 + 2027$	86	0.987
South Atlantic	$(\text{C}_t:\text{N})_r = 9.0 \cdot \text{NO}_3 + 1901$	133	0.957
<i>Nitrogen Versus Phosphorus</i>			
$\sigma_\theta = 26.8 \text{ kg m}^{-3}$			
North Atlantic	$\text{NO}_3 = 16.0 \cdot \text{PO}_4 - 3.2$	74	0.999
South Atlantic	$\text{NO}_3 = 16.0 \cdot \text{PO}_4 - 3.5$	129	1
$\sigma_\theta = 27.2 \text{ kg m}^{-3}$			
North Atlantic	$\text{NO}_3 = 15.8 \cdot \text{PO}_4 - 2.4$	86	0.999
South Atlantic	$\text{NO}_3 = 16.1 \cdot \text{PO}_4 - 3.6$	133	1

finding is consistent with that of previous studies [e.g., *Takahashi et al.*, 1985]. However, the N:P regeneration ratios are in surprisingly reasonable agreement with the model underlying ratio. However, nitrate and phosphate cycling is rather simple in the AAMOC model as denitrification is not considered.

4.2. Multiple Linear Regression Method (M1b)

[34] The multiple linear regression method is applied to the interpolated data as well as to the data in T/S and latitudinal classes given by *Li and Peng* [2002] for the Atlantic Ocean. The results for the two isopycnals are summarized in Table 4. Very good agreement of analyzed and AAMOC prescribed RR is found on isopycnal 27.2 kg m^{-3} in the South Atlantic. As we will show later with the aid of the mixing analysis, this isopycnal is dominated by a single southern outcrop/end member characteristic up to 15°N . Results for the North Atlantic deviate from the prescribed RR and we account this to be the result of the rather complex ventilation of the North Atlantic lower thermocline from three sources: NACW, SACW, and MW. Although M1b does not need explicitly defined end member characteristics,

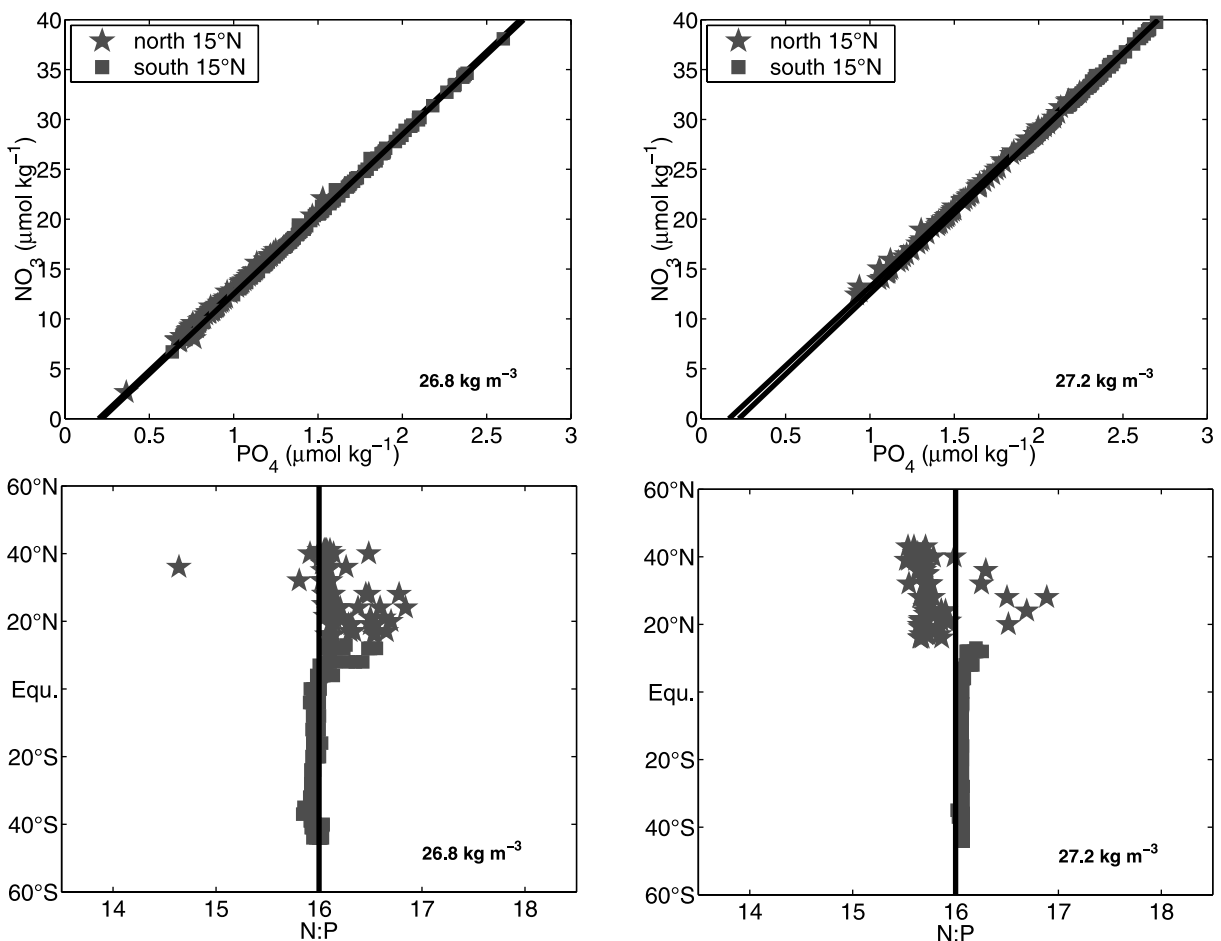


Figure 4. (top) Regression lines (M1a) of modeled nitrogen (NO_3) versus phosphate (PO_4) concentrations from the (left) $\sigma_\theta = 26.8 \text{ kg m}^{-3}$ and (right) $\sigma_\theta = 27.2 \text{ kg m}^{-3}$ isopycnals. The black lines show the slopes of the regression lines (reduced major axis) for data from the North Atlantic (stars) and South Atlantic (squares), respectively. (bottom) N:P plotted versus latitude.

Table 4. $C_{org}:N:P$ Ratios From the Multiple Linear Regressions Method in the North (North of 15°N) and South (South of 15°N) Atlantic on the Two Isopycnals $\sigma_{\theta} = 26.8 \text{ kg m}^{-3}$ and $\sigma_{\theta} = 27.2 \text{ kg m}^{-3}$

	Remineralization Ratio	
	$C_{org}:N$	$N:P$
$\sigma_{\theta} = 26.8 \text{ kg m}^{-3}$		
North Atlantic	5.4	16.7
South Atlantic	6.0	15.9
Atlantic (50° S to 40° N)	6.1	16.1
$\sigma_{\theta} = 27.2 \text{ kg m}^{-3}$		
North Atlantic	5.7	16.6
South Atlantic	6.4	16.0
Atlantic (50°S to 40°N)	6.7	16.0

it probably suffers from the assumption of a maximum of three end members. This is in particular true if one analyzes subvolumes within an ocean basin, as *Li and Peng* [2002] did. Each of the subvolumes is assumed to be composed from a maximum of three end members. Although the T/S relation in the subvolumes may apparently support a three end member mixing assumption, one has to keep in mind that each interior point in the ocean is a composition of water masses from multiple sources; each of them has its own “history” [Tomczak, 1999]. Hence what M1b assumes to be an end member is already a mixing product of a number of end members with different remineralization stages. The analysis of the AAMOC model data following the T/S classes as suggested by *Li and Peng* [2002] show such apparent changes in regeneration ratios (Figure 5). *Li and Peng* [2002] interpreted their results as a change in remineralization ratios along the “global ocean conveyor belt route” from the Atlantic into the Indian and Pacific oceans. However, following a water parcel along the route, it carries more and more contributions of other, unresolved end members, which leads to a change in the

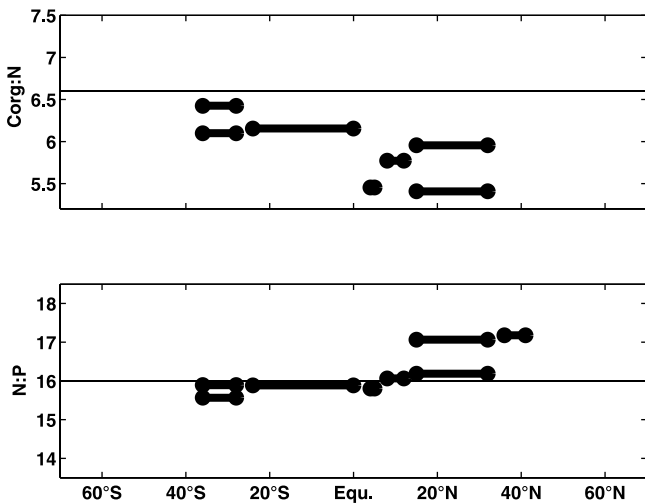


Figure 5. Multiple linear regression method applied to AAMOC data following the spatial separation given by *Li and Peng* [2002].

analyzed remineralization ratios. Consequently, the assumption of analyzing “real” end member values is no longer valid.

[35] In summary, the M1b method gives good results for situations where mixing does not play much of a role. Although it does not rely on explicit end member definitions, only a maximum of three end members are allowed to mix. Mixing of already modified water masses results in alterations of the reconstructed remineralization ratios (Figure 5).

4.3. Mixing Triangle Approach (M2a)

[36] The M2a approach considers mixing of the three end members NACW, SACW, and MW on isopycnals 26.8 and 27.2 kg m^{-3} . On the 26.8 kg m^{-3} isopycnal NACW and SACW almost exclusively mix with only minor contributions of a few percent of MW (Figure 6). North of about 15°N the method predicts water masses dominated by NACW. In the latitudes from 10°S to 15°N, a broad range

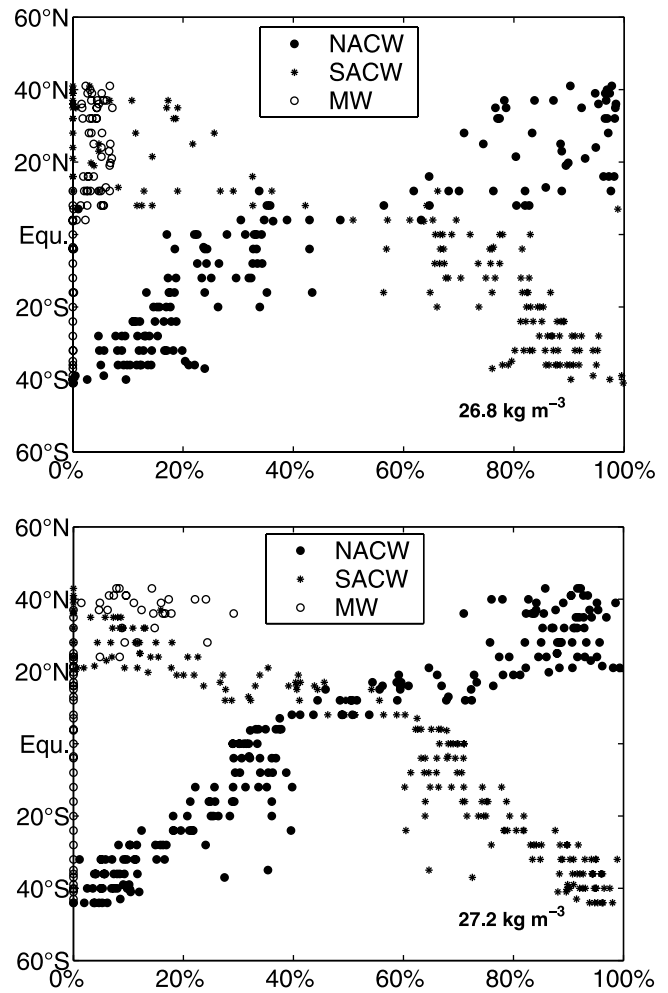


Figure 6. Contributions of different source waters to water mass mixing (M2a) at each station in the Atlantic Ocean for the (top) $\sigma_{\theta} = 26.8 \text{ kg m}^{-3}$ isopycnal and (bottom) $\sigma_{\theta} = 27.2 \text{ kg m}^{-3}$ isopycnal. NACW, North Atlantic Central Water; SACW, South Atlantic Central Water; MW, Mediterranean Water.

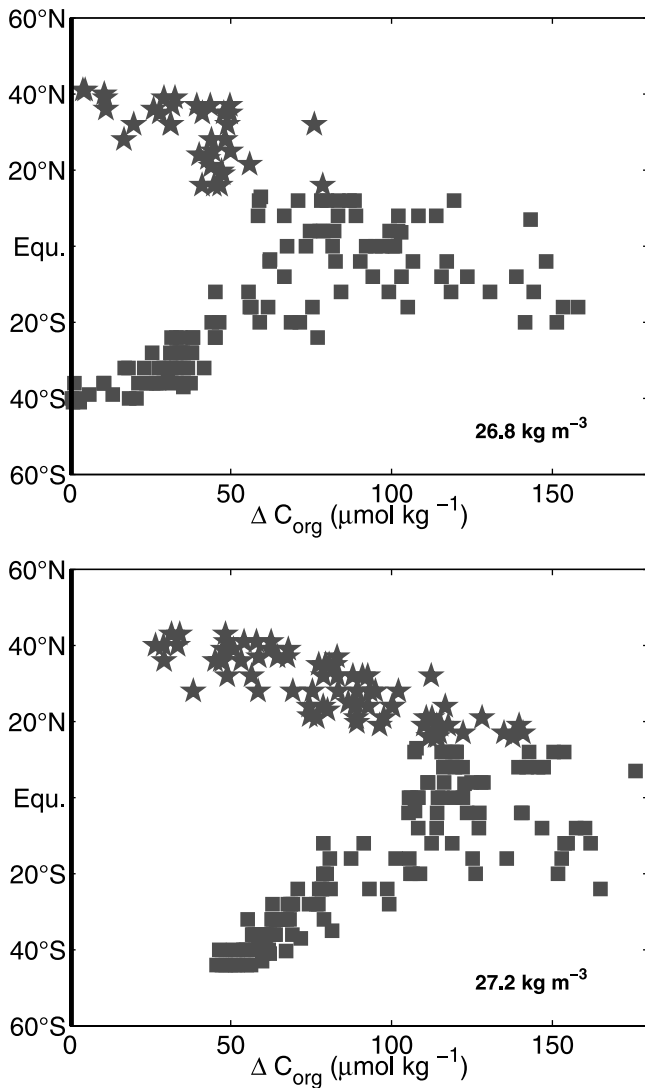


Figure 7. Organic carbon regeneration rates (ΔC_{org}) on the (top) $\sigma_{\theta} = 26.8 \text{ kg m}^{-3}$ isopycnal and (bottom) $\sigma_{\theta} = 27.2 \text{ kg m}^{-3}$ isopycnal, obtained by M2a. The stars denote data north of 15°N ; squares show data south of 15°N .

of mixtures between NACW and SACW can be found, with NACW contributions ranging from 30 to 90%. It is interesting to note that even north of the equator, SACW still contributes up to 70% to the water mass composition. South of the equator, SACW contributions prevail and increase almost linearly toward the south. However, even at about 30°S to 40°S , we still find 10 to 20% of NACW. On the 27.2 kg m^{-3} isopycnal the general mixing pattern is similar to the one on 26.8 kg m^{-3} . The main difference is that between 25°N and 50°N the contribution of MW reaches up to 30% of the North Atlantic water mass composition (Figure 6).

[37] Ideally, the mixing of preformed (end member) DIC and NO_3 as well as preformed NO_3 and PO_4 concentrations for each model grid point should lie within a triangle between the three respective end member concentrations. Although not shown here, this is fulfilled for almost all data

points on both isopycnals. As expected, the concentrations of DIC, NO_3 , and PO_4 continuously increase from their outcrop regions toward the equator, showing an integrated signal of biological remineralization toward lower latitudes (Figure 7). Highest remineralization does not occur at the equator but along the eastern boundary of the Atlantic subtropical gyres as expected from the gyre ventilation theory [Luyten *et al.*, 1983] and also from satellite-based estimates of primary and new production [Antoine *et al.*, 1996; Laws *et al.*, 2000].

[38] The $C_{org}:\text{N}$ (Figure 8) and N:P remineralization ratios (Figure 9) yielded by the M2a method agree reasonably well with the AAMOCC model prescribed values. On the 26.8 kg m^{-3} isopycnal we obtain a mean $C_{org}:\text{N}$ ratio of 6.4 ($s = 1.4$, $n = 149$) and a N:P ratio of 15.6 ($s = 0.7$, $n = 151$). Results on the 27.2 kg m^{-3} isopycnal are slightly better with a

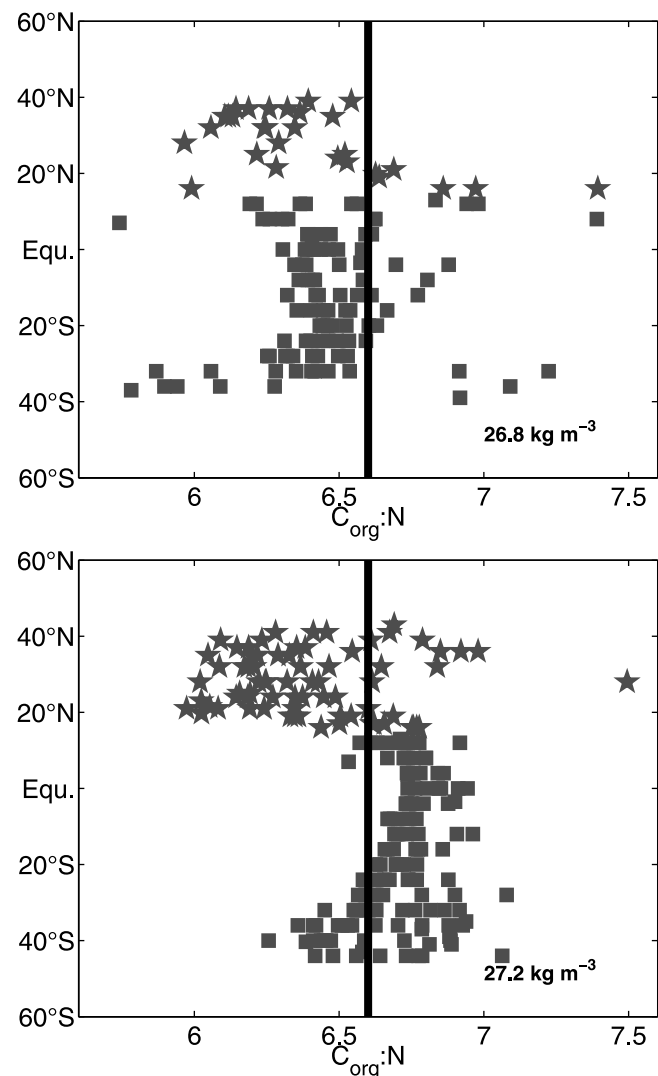


Figure 8. $C_{org}:\text{N}$ regeneration ratios determined by the mixing method M2a for the (top) $\sigma_{\theta} = 26.8 \text{ kg m}^{-3}$ and (bottom) $\sigma_{\theta} = 27.2 \text{ kg m}^{-3}$ isopycnal, respectively. The stars denote data north of 15°N ; squares show data south of 15°N .

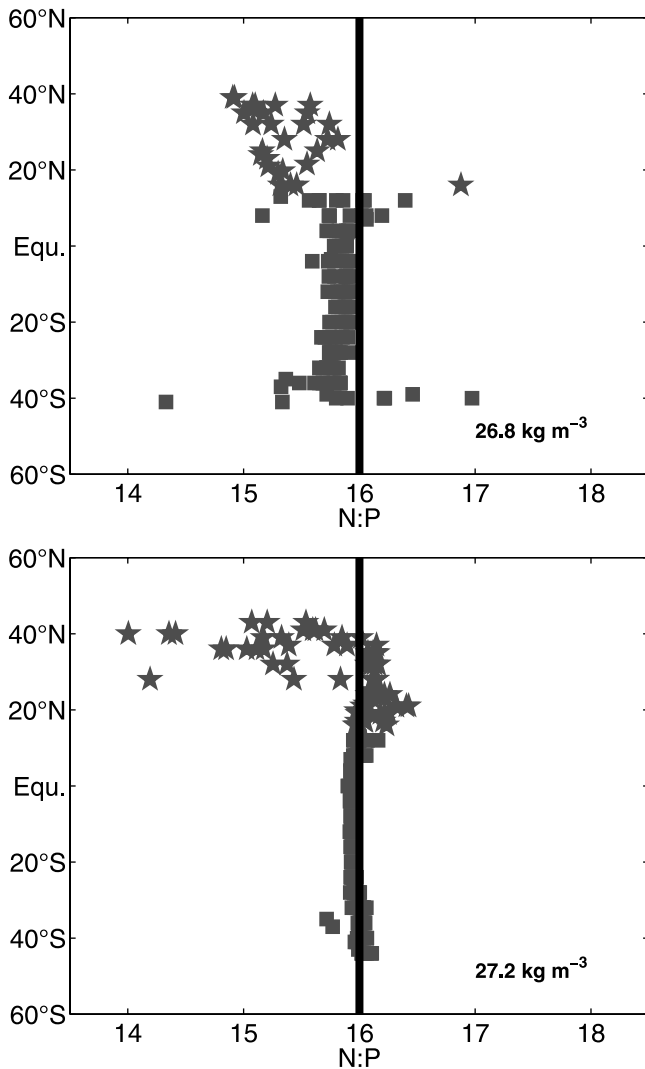


Figure 9. N:P regeneration ratios determined by the mixing method M2a for the (top) $\sigma_{\Theta} = 26.8 \text{ kg m}^{-3}$ and (bottom) $\sigma_{\Theta} = 27.2 \text{ kg m}^{-3}$ isopycnal, respectively. The stars denote data north of 15°N ; squares show data south of 15°N .

mean $C_{org}:\text{N}$ ratio of 6.7 ($s=0.4$, $n=214$) and a corresponding N:P ratio of 15.9 ($s=0.3$, $n=214$). However, there is considerable scatter, and a Student's T-test reveals slight but significant ($p < 0.05$) deviations from the AAMOC model prescribed ratios (which are treated as fixed values without standard deviations on their own) for all of the reconstructed average $C_{org}:\text{N}$ and N:P ratios. In general, the best agreement between AAMOC model and the reconstructed ratios is found in the low latitudes, where the total regeneration signal is highest (Figure 7).

[39] The M2a results are sensitive to the predefined nutrient and DIC end members (source water types) and, via the mixing ratios (fractions variability), to the predefined temperature and salinity end members. To test the sensitivity of our results, we analyze 1000 realizations of the data set modified through a random noise of 5% in the assumed

nutrient and DIC end member concentrations (see Table 2). First, all tracers and end members are varied simultaneously, and second, the perturbations are performed separately for the individual end member and tracer. For each random variation, the resulting regeneration ratios are determined and their deviations from the respective RR used by the model are plotted versus the randomly varied end member concentrations. Best fits of these regressions should result in an optimized end member value for each water mass and tracer. It turns out that using end member values optimized in this way always leads to considerably larger deviations between the modeled and the reconstructed regeneration ratios. This indicates that our initial end member definition represents the optimal solution.

[40] For the first test of varying all end members at the same time, a worsening of results can be explained by the fact that one “optimized” end member, for example, the DIC value for NACW, is not necessarily achieved by using the respective optimized DIC end member for SACW. In the second case of individual SWT variations, the optimization of any further end member always tries to reduce possible misfits from other estimates of SWT, which are probably generated through their systematic variation, before. Therefore, iteratively varying all end members separately even leads to a growing divergence of the “optimized” and “true” regeneration ratios. For example, average $C_{org}:\text{N}$ regeneration ratios on the 26.8 kg m^{-3} isopycnal range between 0.6 and 11.4 for $\pm 50 \mu\text{mol kg}^{-1}$ DIC variations (2.5%) of NACW or SACW. Less sensitivity is found for uncertainty in nitrate end member concentrations, where variations of $\pm 0.5 \mu\text{mol kg}^{-1}$ (4–8%) either in NACW or SACW lead to average $C_{org}:\text{N}$ ratios ranging from 3.2 to 6.7 and to average N:P ratios between 14.9 and 16.6. However, one also has to consider regional deviations of the reconstructed regeneration ratios. During the random SWT variation, apparently suitable average regeneration ratios can be obtained despite strong meridional gradients, for example, when ratios in the North Atlantic are highly overestimated while ratios in the South Atlantic are underestimated, correspondingly.

[41] To investigate the sensitivity of the calculated mixing contributions to the chosen end member characteristics (SWT) of T and S, those end member values are chosen to span the entire range of values in the T/S-diagram. The resulting mixing pattern does not lead to noticeable changes in the South Atlantic mixing contributions, but in the North Atlantic a distinctly higher and northward increasing contribution of SACW is found. However, using the thus obtained mixing fractions, and a further optimization of DIC and nutrient end member values by random variations, again leads to larger deviations from the modeled regeneration ratios than using the initially determined end members for T, S, DIC, and nutrients.

[42] In short, all efforts of varying T and S as well as DIC and nutrient end member concentrations have shown that the determination of regeneration ratios is sensitive even to small changes in the end member values. Reconstructed regeneration ratios are particularly sensitive in the high latitudes, and results are more robust in the low latitudes, i.e., away from the outcrop regions. Although only model

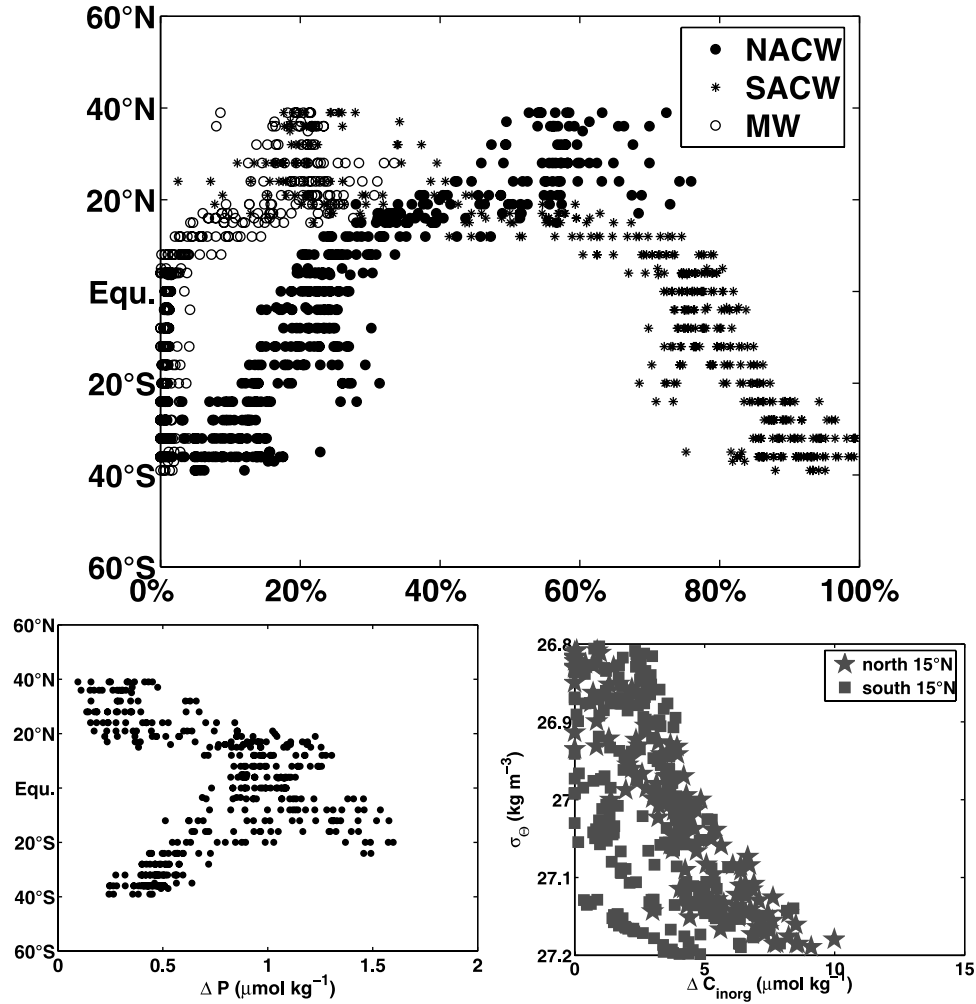


Figure 10. (top) Water mass mixing for the AAMOC Atlantic model domain in the M2b approach, covering the density interval from $\sigma_{\theta} = 26.8 \text{ kg m}^{-3}$ and $\sigma_{\theta} = 27.2 \text{ kg m}^{-3}$. NACW, North Atlantic Central Water; SACW, South Atlantic Central Water; MW, Mediterranean Water. (bottom left) Corresponding phosphate regeneration rates. (bottom right) CaCO_3 dissolution.

generated data are used, which provide an “ideal” data set with good data coverage and without measurement errors or anthropogenic CO_2 contamination, i.e., with all conceptual requirements being fulfilled at the best, in our study the M2a-method is still unable to satisfactorily reproduce the AAMOC model regeneration ratios at all latitudes.

4.4. OMP Analysis Approach (M2b)

[43] The main difference between the mixing triangle approach (M2a) and the OMP analysis approach (M2b) is that M2b determines the effect of mixing (f) and biogeochemical processes (remineralization/respiration ΔP , calcium carbonate dissolution ΔC_{CaCO_3}) in a single step, using all available tracers at a given data point, simultaneously [Karstensen and Tomczak, 1998; Hupe and Karstensen, 2000]. We applied M2b to the isopycnal data as well as to all data between 26.8 kg m^{-3} and 27.2 kg m^{-3} . In total seven tracers (T, S, NO_3 , PO_4 , O_2 , TALK, DIC) plus the mass conservation constraint ($\sum f = 1$) are utilized for the analysis. This set of tracers allows to resolve mixing

of five SWT (two for each of the NACW and SACW, and one for MW) plus two biogeochemical modifications (ΔP and ΔC_{CaCO_3}) and it still allows to solve the system considering the non-negative water mass fractions. Results presented here are based on a set of 25 realizations of the analysis with modifications of the SWT values through random noise, to account for sensitivity of the results on uncertainties in SWT matrix. Normalized random noise is multiplied by a factor for each tracer (T: 0.1° ; S: 0.1 psu ; O_2 : $1 \mu\text{mol kg}^{-1}$; PO_4 : $0.01 \mu\text{mol kg}^{-1}$; NO_3 : $0.5 \mu\text{mol kg}^{-1}$; ALK: $1 \mu\text{mol kg}^{-1}$; DIC: $1 \mu\text{mol kg}^{-1}$). In addition to the uncertainties in the SWT values the OMP results depend to some extent on the choice of the first-guess remineralization ratios ($r_{\text{parameter}/P}$ in equation (5)). At the end of this section an estimate of the effect will be given.

[44] The water mass distribution over the whole density range between 26.8 to 27.2 kg m^{-3} is only little different from that of the M2a approach (Figure 10) on the upper and lower bounding isopycnal. South of 30°S the SACW dominates the water mass structure. Farther north the

influence of the NACW increases and is about 25% between 10°S and 10°N. A transition zone again is between 10°N and 20°N where the NACW contribution increases further to about 60% while MW increases to about 15%; the rest is made up by SACW (25%). Only a few points in the order of 100% NACW can be found in the North Atlantic. This is not such a surprise as the North Atlantic would be better defined by eastern and western North Atlantic Central Waters [Emery and Meincke, 1986]. The definition we choose is more on the western NACW side, and hence it is more saline than the eastern NACW. As a consequence, the OMP analysis determines a lack of low salinity water in the east and adds contributions from the lower salinity SACW to compensate for it. However, the Atlantic Central Waters are in general not as different in their outcrop characteristics or SWT values (see Table 1).

[45] The integrated remineralized phosphate (ΔP , Figure 10, bottom left plot) is quite similar to the M2a methods findings, again with highest values associated with the sluggish ventilated eastern boundary zones. The inorganic carbon regeneration (ΔC_{CaCO_3} , Figure 10, bottom right plot) has maximum values up to 10 $\mu\text{mol kg}^{-1}$ at about 1000 m depth. This is in agreement with the results from Chung *et al.* [2003], who found substantial dissolution of calcite above the 100% saturation horizon, which is typically below 3000 m depth in the Atlantic Ocean.

[46] The $C_{org}:N$ and $N:P$ remineralization ratios obtained from M2b (Figure 11) match the prescribed AAMOCC ratios best between 20°N and 20°S. Overall average ratios are $C_{org}:N = 6.58$ ($s = 0.53$, $n = 20900$) and $N:P = 16.26$ ($s = 1.39$, $n = 20900$). Focusing on the latitude range 20°N to 20°S the average ratios are $C_{org}:N = 6.61$ ($s = 0.05$, $n = 7800$) and $N:P = 16.02$ ($s = 0.23$, $n = 7800$).

[47] The deviations from the prescribed ratios are again strongest toward the outcrop regions. This suggests, as mentioned before, that the quality of the derived ratios increases with the time integrated amount of remineralized substance. In both hemispheres the estimated $N:P$ ratio near the outcrop regions is systematically lower than the prescribed ratio. The estimated $C_{org}:N$ ratio fits the prescribed value quite well, but there are outliers toward higher ratios in the Northern Hemisphere and toward lower ratios in the Southern Hemisphere. We suspect uncertainties in the SWT matrix, possibly as a result of spatial gradients in the outcrop region, as the most likely reason for the deviations. For example, if one defines the nitrate SWT too low, the water away from the outcrop will always be analyzed as slightly too high in remineralized nitrate. Near the outcrop, where the remineralization signal is low, such overestimated remineralized nitrate weights stronger on the overall signal and, assuming source water values for phosphate and carbon to be “correct,” results in too low $C_{org}:N$ and too high $N:P$ ratios. As the southern $C_{org}:N$ scatters mainly at the outcrop latitude (40°S), we assume that the carbon SWT is on the high side of the outcrop surface waters. The nitrate SWT is reasonable and, owing to the too low $N:P$ ratio, we conclude that the PO_4 SWT value is underestimated as well. The same is true for the Northern Hemisphere, except that the carbon SWT value is on the lower side of the outcrop surface water concentrations.

[48] As already mentioned, the M2b analysis needs a set of first guess remineralization ratios ($r_{parameter/P}$ etc., in equation (5)) to connect the tracers affected through remineralization/respiration. Hupe and Karstensen [2000] deduced an “optimized set” of remineralization ratios from observational data through repeat analysis adapting in each analysis the ratio obtained from the former analysis. We attempt to follow this strategy, but it turns out that the AAMOCC model data converge to different values than those prescribed ($C_{org}:N = 6.3$ and $N:P = 15.6$). This might well result again from uncertainties in the SWT values. Therefore we further investigate how the tracer residuals react to systematic changes of each first-guess ratio, say $N:P$. The first guess $N:P$ ratio is varied from 15.5 to 16.5 and the changes in the root mean square of the N and P normalized residuals are investigated (Figure 12). The lowest RMS of the respective tracer pair is found for the prescribed AAMOCC model ratios, offering an alternative way to find the best ratios. However, it should be mentioned that the results are again sensitive to the choice of SWT values and emphasizing again the importance of “accurate” SWT (end member) definitions.

5. Discussion

[49] In order to estimate the remineralization ratios from observational data, different approaches have been used in the past. Four of the methods are tested here: Two methods use linear regressions without predefinition of end members that compose the interior tracer field (M1a, M1b), and two need end members to be defined (M2a, M2b).

[50] Estimating remineralization ratios by simply calculating the regression equations of DIC versus NO_3 (M1a, Figures 3 and 4) has shown that generally the reconstruction of $C_{org}:N$ is poor, especially on the 27.2 kg m^{-3} isopycnal, whereas $NO_3:PO_4$ regressions fit the model immanent ratio of 16, quite well (Table 3). One reason for the inconsistency between remineralization ratios estimated by M1a and those actually prescribed in the AAMOCC model lies in the mixing of water masses with different preformed DIC and NO_3 values. Absolute DIC and, in particular, nitrate concentrations in the South Atlantic, which belongs to the “high nutrient low chlorophyll” (HNLC) [Cullen, 1991] region of the Southern Ocean, are higher than in the North Atlantic with absolute $DIC:NO_3$ ratios being higher in the north (Tables 1 and 2). Consequently, the influence of the high nutrient water from the south will lead in the North Atlantic to the less steep slope of isopycnal $DIC:NO_3$ ratios. Conversely, in the South Atlantic, mixing of water from the north, which is relatively rich in DIC (if compared to nitrogen content), leads to a steeper slope of the $DIC:NO_3$ regression there. However, this mechanism explains probable mixing effects only qualitatively, but not quantitatively, and it shows that it is not suitable to use a single correction equation for the whole Atlantic Ocean. Moreover, mixing is not necessarily restricted to isopycnal mixing processes, and effects caused by $CaCO_3$ -dissolution may in principle be included. In contrast, the $N:P$ ratios are merely unaffected by the mixing which would suggest that NO_3 and PO_4 cycling is quite similar in the North and South Atlantic basins of the AAMOCC model.

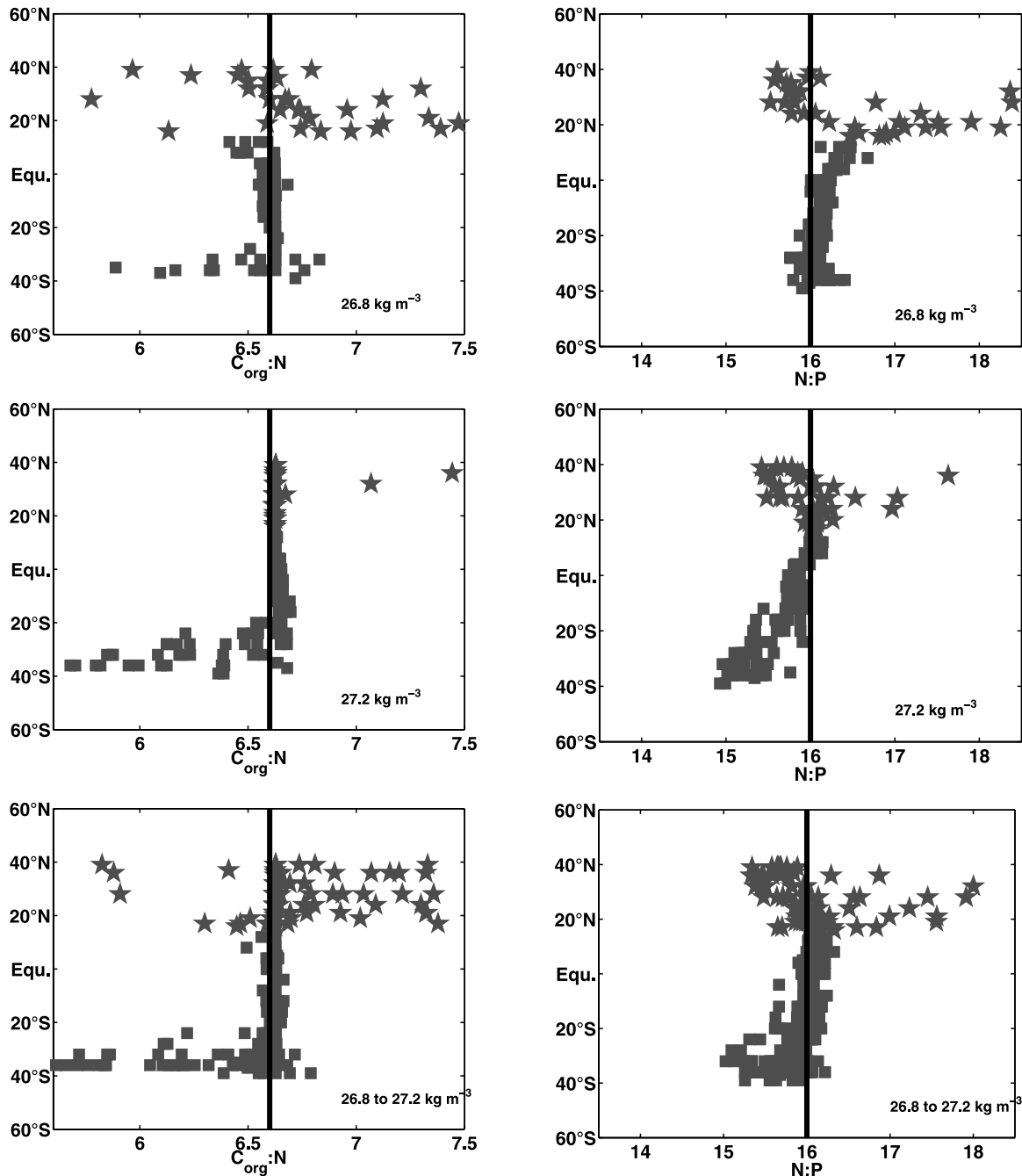


Figure 11. Regeneration ratios for $C_{org}:N$ and $N:P$ as determined by M2b plotted versus latitude for (top) isopycnal data along 26.8 kg m^{-3} , (middle) data along 27.2 kg m^{-3} , and (bottom) all data between 26.8 kg m^{-3} and 27.2 kg m^{-3} . The stars denote data north of 15°N ; squares show data south of 15°N .

[51] In summary, the application of M1a to the AAMOCC model results has shown that changes in the absolute concentrations of DIC, nitrogen, and phosphorus in the Atlantic Ocean, especially increasing concentrations toward lower latitudes, can largely be attributed to biological remineralization (as it is prescribed in the AAMOCC model). It is tempting to use a method like M1a due to its simplicity. Nevertheless, a biasing effect of water mass mixing (isopycnal and diapycnal), even on relatively short

horizontal distances, affects the remineralization ratios, as was derived here from the AAMOCC model data.

[52] Estimating the remineralization ratios from a multiple linear regression (M1b) [Li and Peng, 2002] results in a reasonable agreement when utilizing all data along an isopycnal at once (Table 4). Deviations from the prescribed AAMOCC ratios increase away from the outcrop regions when partitioning the ocean into subregions/subvolumes (as applied by Li and Peng [2002]). Our interpretation of the

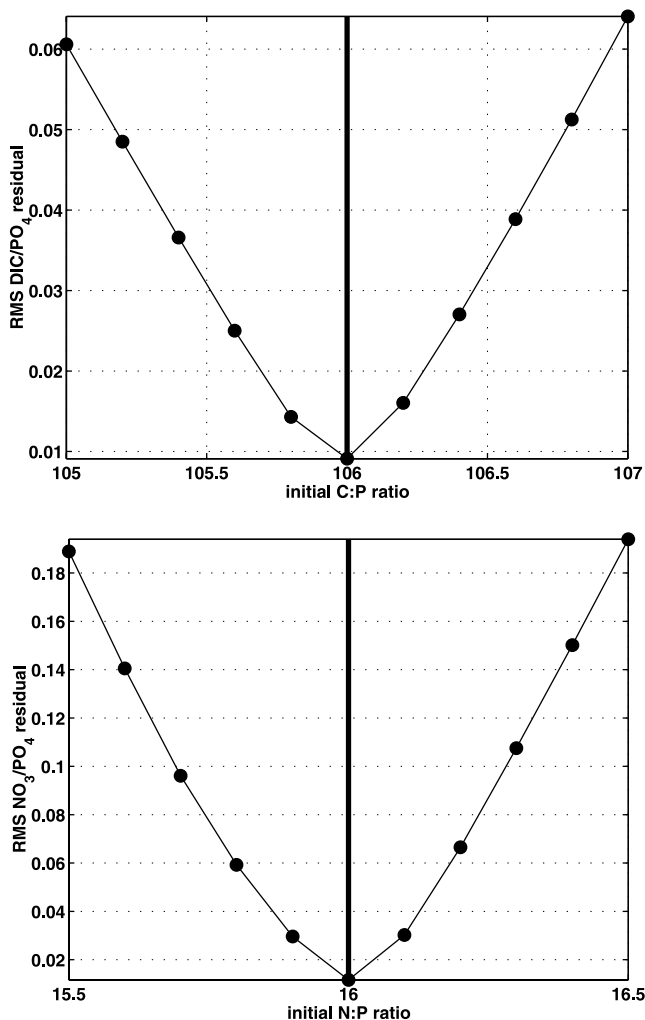


Figure 12. Optimization of first guess Redfield ratios in the M2b approach. Plotted are the mass conservation residuals versus C:P and N:P element ratios of regeneration, showing minimum residuals exactly at the model immanent regeneration ratios ($C_{org}:P$, N:P).

apparent systematic deviation is that M1b assumes a linear mixing of end members while the interior data in a subregion does not contain “real” end members, but are already a mixture of several end members. With increasing signatures of mixing in the data the deduced remineralization ratios tend to be more and more biased from the “real,” in our case, the AAMOCC ratios. For the deep water masses, which have a single source, say in the North Atlantic, the deviation would increase as the water spreads into the Indian and Pacific oceans.

[53] Accounting for water mass mixing using predefined end member characteristics (M2a and M2b) results in more reliable estimates of the AAMOCC prescribed remineralization ratios. With the three end member isopycnal analysis using only T/S to estimate the mixing yields best agreement for the $C_{org}:N$ remineralization ratios in the low latitudes. Even though end members are carefully chosen on the respective isopycnals to find those water masses below

the euphotic zone which have recently been ventilated ($AOU < 40 \mu\text{mol kg}^{-1}$), significant deviations from the AAMOCC model prescribed remineralization ratios are found for large regions in the model Atlantic Ocean. Reasons for these deviations are contributions from diapycnal mixing of source waters, incorrect assumptions on the end member characteristics and assumptions of linear mixing along isopycnals, which are nonlinear through the nonlinearity of the equation of state.

[54] For the upper open ocean the effect of diapycnal mixing can be argued to be strongest in frontal systems with high levels of baroclinic and smaller-scale instability, for example situated at the poleward side of the subtropical gyre. The systematically underestimated $C_{org}:N$ remineralization ratios in the intermediate to high latitudes on both isopycnals, especially on 27.2 kg m^{-3} , may be caused by such processes. A reduction of the calculated $C_{org}:N$ ratio and also the decreasing N:P regeneration ratios in the Northern Hemisphere could be explained by diapycnal input of waters with a low DIC: NO_3 ratio (water that is relatively rich in inorganic nitrogen) and with low $\text{NO}_3:\text{PO}_4$ ratios (water that is relatively rich in inorganic phosphorus). In the model’s North Atlantic, ratios of vertical gradients of DIC and NO_3 show values below the classical Redfield $C_{org}:N$ ratio. This means that NO_3 is increasing more rapidly over depth than DIC with regard to Redfield stoichiometry. Consequently, vertical mixing with relative NO_3 rich water from below can result in the low estimated $C_{org}:N$ remineralization ratios in those regions. In the South Atlantic, however, the modeled ratio of vertical DIC gradients versus vertical NO_3 gradients corresponds to the modeled $C_{org}:N$ (RR) ratio very well.

[55] In the North Atlantic the ratio of vertical NO_3 and PO_4 gradients also corresponds to the Redfield N:P ratio very well; that is, upwelling cannot explain the too low reconstructed $\text{NO}_3:\text{PO}_4$ remineralization ratios there, whereas in the South Atlantic, vertical NO_3 and PO_4 gradients also fit well with the modeled (RR) and reconstructed N:P ratios, especially on the 27.2 kg m^{-3} isopycnal.

[56] The remineralization ratios derived with the M2b approach are rather similar to the results from the M2a approach, yielding good results in the low latitudes and systematic deviations in the higher latitudes. Using the AAMOCC model output with a simple biogeochemical cycling and for the two isopycnals chosen, the M2b approach is superior to M2a for the $C_{org}:N$ ratio (compare Figures 8 and 11), and its application to both data sources, those data interpolated on isopycnals and to the 3-D volume, shows very similar results (Figure 11). Consequently, the discrepancy between results from these different types of methods, as it may appear from the current literature, is not caused by the choice of data, but will be caused by assumptions and/or treatment of water mass mixing and end member definitions. In addition, there are methodological differences among the two approaches that may help to decide whether using a mixing triangle (M2a) or a multiparameter (M2b) approach is advantageous.

[57] 1. M2b is not limited to a maximum of three source water types (SWT; or end members) as M2a is. The maximum number of SWT depends on the number of

tracers available as well as on the numbers of biogeochemical cycling processes to be resolved. This may allow to analyze more data points and thus permits better statistics of the results (as in our example).

[58] 2. M2b derives mixing, remineralized material (ΔP), and CaCO_3 dissolution (ΔC_{CaCO_3}) in a single step of coupled linear equations, whereas M2a solves the equations in two stages (first the mixing fractions, then the remineralization and dissolution). The importance of this difference is in the propagation of errors: In M2a, any errors in the mixing fractions are propagated directly in the ΔP and ΔC_{CaCO_3} estimates, while in M2b the residuals to all the equations are considered in a balanced way.

[59] 3. M2b can be extended to include more biogeochemical cycling processes than only remineralization and CaCO_3 dissolution, for example, denitrification [Hupe and Karstensen, 2000] and the anthropogenic perturbation on DIC.

[60] 4. However, M2b requires and may be sensitive to the use of first guess RR.

[61] With the AAMOCC model output, we have an idealized data set available to test the limitations of individual methods that estimate remineralization ratios. However, the AAMOCC model itself has limitations which simplify our analysis on one hand, but on the other hand may limit the direct transfer of our results to the treatment of “real ocean” observational data. Namely, the effects of denitrification, of “natural” variability (depth and regional) of remineralization ratios, of anthropogenic disturbances (CO_2), and of a nonsteady state of the whole system are all neglected. Their consideration will require different steps to be taken for the different methods, which are likely to display different sensitivities to errors in the representation of these effects.

6. Conclusions

[62] 1. The simple regression method (M1a), that ignores mixing of different water masses with different preformed tracer concentrations, shows a strong signal of changes in DIC, NO_3 , and PO_4 that is largely caused by the remineralization of organic matter. However, especially for $C_{\text{org}}:\text{N}$, these changes are severely biased by effects of mainly isopycnal mixing of water masses with different preformed DIC and nutrient concentrations.

[63] 2. Multiple linear regression (M1b) considers the mixing of three end member characteristics in an indirect way, without the need to define end members. Utilizing all data along an isopycnal, reasonable agreement between calculated and AAMOCC model remineralization ratios is found (Table 4). Dividing the ocean into subvolumes, which are analyzed separately, results in systematic differences. We attribute this to time integrated mixing information that is carried in the interior tracer field. For each subvolume, this method reduces to a system of three end members, which in reality are not “pure” end members, but instead have already been affected by mixing and biogeochemical processes.

[64] 3. Both methods that need predefined end member characteristics (M2a, M2b) adequately reproduce the mod-

eled $C_{\text{org}}:\text{N}$ and $\text{N}:\text{P}$ ratios of remineralization best in the low latitudes (20°N to 20°S). Deviations from the prescribed RR can be explained by uncertainties in the end member characteristics. As a consequence, determination of mixing is highly sensitive to changes in end member assumptions, requiring careful definitions of end member water mass characteristics.

[65] 4. Among the methods investigated, method M2b provides the most consistent way to reconstruct the AAMOCC model immanent regeneration ratios. This indicates that as many independent parameters as possible should be included for the determination of mixing and regeneration ratios. Furthermore, this approach uses a larger database, which permits analysis with greater statistical certainty. When, however, using real observations, additional biogeochemical processes like denitrification and anthropogenic additions to DIC have to be considered.

[66] 5. Overall, it seems fair to say that methods which are based on predefined end member characteristics (M2a, M2b) appear to derive the AAMOCC model remineralization rates better than the linear regression methods (M1a, M1b). However, finding the end member characteristics is not a trivial task, as they have to be picked in the regions where the formation of water masses takes place. All end members defined outside such regions are likely to be influenced already by mixing and may result in alteration on the remineralization ratios (see M1b). Such a “mixing problem” should be true for a variety of biogeochemical cycling studies (e.g., anthropogenic carbon uptake).

[67] 6. All methods applied here find some variability in the reconstructed element ratios for (organic) carbon and nutrient regeneration, which in this study are caused by methodological deficiencies only. When applying these methods to the real ocean, similar variations may erroneously be interpreted as spatial and/or temporal variations of the real remineralization ratios.

[68] 7. The AAMOCC model version used in this study has limitations which simplify our analysis on the one hand, but limit the direct transfer of our results to the treatment of “real ocean” data, owing to the model’s neglect of processes like denitrification, depth and regional variability of remineralization ratios, anthropogenic disturbances (CO_2), and deviations from a steady state ocean.

[69] **Acknowledgments.** We thank Aneurin Henry-Edwards and an anonymous reviewer for their constructive and supporting comments, which helped to improve the quality of this manuscript, significantly. This study was partly financed through the German JGOFS North Atlantic Synthesis program.

References

- Akima, H. (1970), A new method of interpolation and smooth curve fitting based on local procedures, *J. Assoc. Comput. Mach.*, 17(4), 589–602.
- Anderson, L., and J. Sarmiento (1994), Redfield ratios of remineralization determined by nutrient data analysis, *Global Biogeochem. Cycles*, 8(1), 65–80.
- Antoine, D., J. M. André, and A. Morel (1996), Oceanic primary production: 2. Estimation at global scale (coastal zone color scanner) chlorophyll, *Global Biogeochem. Cycles*, 10(1), 57–69.
- Broecker, W. S. (1974), A conservative water-mass tracer, *Earth Planet. Sci. Lett.*, 23, 100–107.
- Buesseler, K. O., A. F. Michaels, D. A. Siegel, and A. H. Knap (1994), A three-dimensional time-dependent approach to calibrating sediment trap fluxes, *Global Biogeochem. Cycles*, 8(2), 179–193.

- Chung, S.-N., K. Lee, R. A. Feely, C. L. Sabine, F. J. Millero, R. Wanninkhof, J. L. Bullister, R. M. Key, and T.-H. Peng (2003), Calcium carbonate budget in the Atlantic Ocean based on water column inorganic carbon chemistry, *Global Biogeochem. Cycles*, *17*(4), 1093, doi:10.1029/2002GB002001.
- Cullen, J. J. (1991), Hypotheses to explain high-nutrient, low chlorophyll conditions in the open sea, *Limnol. Oceanogr.*, *36*, 1578–1599.
- Emery, W. J., and J. Meincke (1986), Global water masses: Summary and review, *Oceanol. Acta*, *9*(4), 383–391.
- Gruber, N. (1998), Anthropogenic CO₂ in the Atlantic Ocean, *Global Biogeochem. Cycles*, *12*(1), 165–191.
- Gruber, N., and J. L. Sarmiento (1997), Global patterns of marine nitrogen fixation and denitrification, *Global Biogeochem. Cycles*, *11*(2), 235–266.
- Holland-Hansen, B. (1918), Nogen hydrografiske metoder, *Forh. Skand. Nat. Mote*, *16*, 357–359.
- Hupe, A., and J. Karstensen (2000), Redfield stoichiometry in the Arabian Sea, *Global Biogeochem. Cycles*, *14*(1), 357–372.
- Intergovernmental Panel on Climate Change (2001), *Climate Change 2001: The Scientific Basis. Contribution of Working Group I to the Third Assessment Report of the Intergovernmental Panel on Climate Change (IPCC)*, edited by J. T. Houghton et al., Cambridge Univ. Press, New York.
- Kähler, P., and E. Bauerfeind (2001), Organic particles in a shallow sediment trap: Substantial loss to the dissolved phase, *Limnol. Oceanogr.*, *46*, 719–723.
- Karstensen, J., and D. Quadfasel (2002), Formation of Southern Hemisphere thermocline waters: Water mass conversion and subduction, *J. Phys. Oceanogr.*, *22*, 3020–3038.
- Karstensen, J., and M. Tomczak (1998), Age determination of mixed water masses using CFC and oxygen data, *J. Geophys. Res.*, *103*(C9), 18,599–18,610.
- Körtzinger, A., J. I. Hedges, and P. D. Quay (2001), Redfield ratios revisited: Removing the biasing effect of anthropogenic CO₂, *Limnol. Oceanogr.*, *46*, 964–970.
- Laws, E. A., P. G. Falkowski, W. O. Smith, and H. Ducklow (2000), Temperature effects on export production in the open ocean, *Global Biogeochem. Cycles*, *14*(4), 1231–1246.
- Lawson, C. L., and R. J. Hanson (1974), *Solving Least Square Problems*, Prentice-Hall, Upper Saddle River, N. J.
- Li, Y.-H., and T.-H. Peng (2002), Latitudinal change of remineralization ratios in the oceans and its implication for nutrient cycles, *Global Biogeochem. Cycles*, *16*(4), 1130, doi:10.1029/2001GB001828.
- Luyten, J., J. Pedlosky, and H. Stommel (1983), The ventilated thermocline, *J. Phys. Oceanogr.*, *13*, 292–309.
- Marshall, J. C., J. G. Nurser, and R. G. Williams (1993), Inferring the subduction rate and period over the North Atlantic, *J. Phys. Oceanogr.*, *23*, 1315–1329.
- Martin, J. H., G. A. Knauer, D. M. Karl, and W. W. Broenkow (1987), VERTEX: Carbon cycling in the northeast Pacific, *Deep Sea Res.*, *34*, 267–286.
- Minster, J., and M. Boulahdid (1987), Redfield ratios along isopycnal surfaces—A complementary study, *Deep Sea Res.*, *34*, 1981–2003.
- Moran, S. B., M. A. Charette, S. M. Pike, and C. A. Wicklund (1999), Differences in seawater particulate organic carbon concentration in samples collected using small- and large-volume methods: The importance of DOC adsorption to the filter blank, *Mar. Chem.*, *67*, 33–42.
- Noji, T., K. Børsheim, F. Rey, and R. Nortvedt (1999), Dissolved organic carbon associated with sinking particles can be crucial for estimates of vertical carbon flux, *Sarsia*, *84*, 129–135.
- Oschlies, A., and P. Kähler (2004), Biotic contribution to air-sea fluxes of CO₂ and O₂ and its relation to new production, export production, and net community production, *Global Biogeochem. Cycles*, *18*, GB1015, doi:10.1029/2003GB002094.
- Pearson, K. (1901), On lines and planes of closest fit to systems of points in space, *Philos. Mag.*, *6*(2), 559–572.
- Redfield, A. C., B. C. Ketchum, and F. A. Richards (1963), The influence of organisms on the composition of sea water, in *The Sea*, vol. 2, edited by N. Hill, pp. 26–77, Wiley-Interscience, Hoboken, N. J.
- Schlitzer, R. (2000), Applying the adjoint method for global biogeochemical modeling, in *Inverse Methods in Biogeochemical Cycles*, *Geophys. Monogr. Ser.*, vol. 114, edited by P. Kasibhatla et al., pp. 107–124, AGU, Washington, D. C.
- Schlitzer, R. (2002), Carbon export fluxes in the Southern Ocean: Results from inverse modeling and comparison with satellite based estimates, *Deep Sea Res., Part II*, *49*, 1623–1644.
- Schneider, B., R. Schlitzer, G. Fischer, and E.-M. Nöthig (2003), Depth-dependent elemental compositions of particulate organic matter (POM) in the ocean, *Global Biogeochem. Cycles*, *17*(2), 1032, doi:10.1029/2002GB001871.
- Scholten, J. C., J. Fietzke, M. M. Rutgers van der Loeff, A. Mangini, W. Koeve, P. Stoffers, A. Antia, S. Neuer, and J. Wanick (2001), Trapping efficiencies of sediment traps from the deep eastern North Atlantic: The ²³⁰Th calibration, *Deep Sea Res., Part II*, *48*, 2383–2408.
- Shaffer, G., J. Bendtsen, and O. Ulloa (1999), Fractionation during remineralization of organic matter in the ocean, *Deep Sea Res., Part II*, *46*, 185–204.
- Siegenthaler, U., and J. Sarmiento (1993), Atmospheric carbon dioxide and the ocean, *Nature*, *365*, 119–125.
- Suess, E. (1980), Particulate organic carbon flux in the ocean—Surface productivity and oxygen utilization, *Nature*, *280*, 260–263.
- Sverdrup, H. U., M. W. Johnson, and R. H. Fleming (1942), *The Oceans: Their Physics, Chemistry, and General Biology*, Prentice-Hall, Upper Saddle River, N. J.
- Takahashi, R. H., T. Wanninkhof, R. A. Feely, R. F. Weiss, D. W. Chipman, N. R. Bates, J. Olafsson, C. L. Sabine, and S. G. Sutherland (1999), Net sea-air CO₂ flux over the global oceans: An improved estimate based on the sea-air pCO₂ difference, in *Proceedings of the Second International Symposium, CO₂ in the Oceans (ISSN 1341-4356)*, edited by Y. Nojiri, pp. 9–14, Cent. for Global Environ. Res. (NIEST), Tsukuba, Japan.
- Takahashi, T., W. S. Broecker, and S. Langer (1985), Redfield ratio based on chemical data from isopycnal surfaces, *J. Geophys. Res.*, *90*(C4), 6907–6924.
- Tomczak, M. (1999), Some historical, theoretical and applied aspects of quantitative water mass analysis, *J. Mar. Res.*, *57*, 275–303.
- Wallace, D. W. R. (2001), Storage and transport of excess CO₂ in the oceans: The JGOFS/WOCE Global CO₂ Survey, in *Ocean Circulation and Climate*, edited by J. Church, G. Siedler, and J. Gould, pp. 489–521, Elsevier, New York.
- Weiss, R. F. (1970), On the solubility of nitrogen, oxygen and argon in water and seawater, *Deep Sea Res.*, *17*, 721–735.
- You, Y., and M. Tomczak (1993), Thermocline circulation and ventilation in the Indian Ocean derived from water mass analysis, *Deep Sea Res.*, *40*, 13–56.

J. Karstensen, Leibniz-Institut für Meereswissenschaften, Düsternbrooker Weg 20, D-24105 Kiel, Germany.

A. Oschlies, School of Ocean and Earth Science, Southampton Oceanography Centre, Southampton SO14 3ZH, UK.

R. Schlitzer, Alfred Wegener Institut für Polar- und Meeresforschung, PF 120161, D-27515 Bremerhaven, Germany.

B. Schneider, Institut für Geowissenschaften, Ludewig-Meyn-Strasse 10, D-24098 Kiel, Germany. (birgit@passagen-uni-kiel.de)